

Game-theoretic Understanding of Adversarially Learned Features

Jie Ren^{* 1} Die Zhang^{* 1} Yisen Wang^{* 2} Lu Chen¹ Zhanpeng Zhou¹ Xu Cheng¹ Xin Wang¹ Yiting Chen¹
Jie Shi³ Quanshi Zhang¹

Abstract

This paper aims to understand adversarial attacks and defense from a new perspective, *i.e.* the signal-processing behaviors of DNNs. We novelly define the multi-order interaction in game theory, which satisfies six properties. With the multi-order interaction, we discover that adversarial attacks mainly affect high-order interactions to fool the DNN. Furthermore, we find that the robustness of adversarially trained DNNs comes from category-specific low-order interactions. Our findings provide more insights into and make a revision of previous understanding for the shape bias of adversarially learned features. Besides, the multi-order interaction can also explain the recoverability of adversarial examples.

1. Introduction

Adversarial robustness of deep neural networks (DNNs) has received increasing attention in recent years. Related studies include adversarial defense and attacks (Szegedy et al., 2013; Carlini & Wagner, 2017). In terms of defense, adversarial training is an effective and the most widely-used method (Goodfellow et al., 2014; Madry et al., 2018).

In spite of the fast development of adversarial attacks and defense, the essential mechanism of the adversarial robustness is still unclear. Thus, the understanding of adversarial attacks and defense is an emerging direction in recent years. Ilyas et al. (2019) demonstrated that adversarial examples could be directly attributed to the presence of non-robust yet discriminative features. Gilmer et al. (2018); Weng et al. (2018) proved an upper bound for the model robustness. Zhang & Zhu (2019) found that adversarial training helped DNNs learn a more interpretable (more shape-biased) representation. Besides the feature interpretability, Tsipras et al. (2018) further showed an inherent tension between the adversarial robustness and the generalization power. These explanations for adversarial attacks and defense are mainly based on the observation of semantic saliency of features, or the proof of the bound for the robustness and generalization.

Beyond above perspectives for explanations, this study aims to explore the essential reason why and how adversarial examples emerge. Specifically, we rethink the adversarial robustness from the novel perspective of interactions between input variables of a DNN. In fact, our research group led by Dr. Quanshi Zhang has proposed game-theoretic interactions, including interactions of different orders (Zhang et al., 2020) and multivariate interactions (Zhang et al., 2021c). As basic metrics, the interaction can be used to explain signal processing in trained DNNs from different perspectives. For example, we have build up a tree structure to explain the hierarchical interactions between words in NLP models (Zhang et al., 2021a). We have also used interactions to explain the generalization power of DNNs (Zhang et al., 2021b). The interaction can also explain the adversarial transferability of adversarial perturbations (Wang et al., 2021). As an extension of the system of game-theoretic interactions, in this study, we explain adversarial attacks and defense based on interactions.

Surprisingly, the interaction provides us with a unified explanation for various aspects of adversarial robustness *w.r.t.* ℓ_∞ untargeted and targeted attacks.

(1) We investigate the distinctive signal-processing behavior when the DNN handles adversarial examples *w.r.t.* normal cases when the DNN deals with normal samples.

^{*}Equal contribution . This study is conducted under the supervision of Dr. Quanshi Zhang, who is with the John Hopcroft Center and MoE Key Lab of Artificial Intelligence AI Institute, Shanghai Jiao Tong University, Shanghai, China. ¹Shanghai Jiao Tong University
²Peking University ³Huawei International. Correspondence to: Quanshi Zhang <zqs1022@sjtu.edu.cn>.

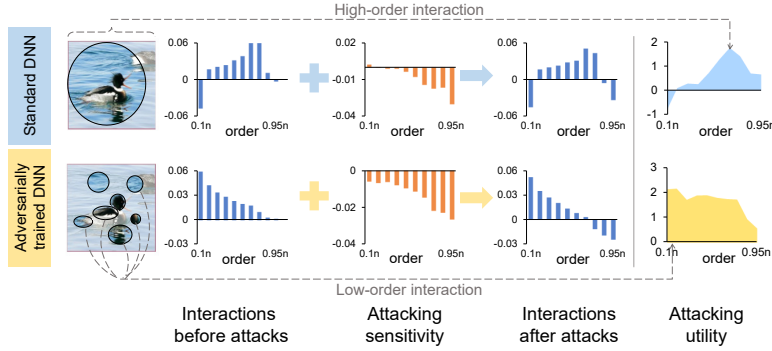


Figure 1. We find that adversarial attacks mainly affect high-order interactions in input samples. Besides, high-order interactions in adversarially trained DNNs are more robust than those in standard DNNs, due to the disentanglement of low-order interactions.

(2) Above investigation also provides a new perspective to understand the difference between adversarial training and standard training, *i.e.* exploring which types of features are sensitive to adversarial perturbations, and the reason why adversarially learned features are robust.

(3) Our research explains the recoverability of adversarial examples to normal samples. Besides, it also explains the essential mechanism of the attribution-based method (Yang et al., 2019) of detecting adversarial examples.

The starting point of all above findings, which makes us rethink adversarial robustness, is the following discovery. When we quantify interactions between input variables of a DNN, we find that the interaction behavior of handling adversarial examples is significantly different from the interaction behavior of dealing with normal samples. The interaction metric also explains the difference between adversarial training and standard training. Specifically, we extend the Shapley interaction index (Grabisch & Roubens, 1999) to the multi-order interaction, in order to explain the adversarial robustness. We can simply understand the interaction between two input variables (i and j), *e.g.* two pixels or two words, as follows. Let $\phi(i)$ denote the importance of the variable i to the network output. The interaction between variables (i, j) is defined as the influence of the presence and absence of the variable j on $\phi(i)$. We further define the order of the interaction, which reflects the contextual complexity of the interaction between i and j . Mathematically, low-order interactions are defined to represent simple features of local collaborations (under simple and local contexts), and high-order interactions indicate complex features of global collaborations (under complex and global contexts). This is also demonstrated by visualization results.

We first prove that the output score of a DNN can be decomposed into the sum of multi-order interactions between different pairs of input variables. Thus, we can explain adversarial effects on the network output, by decomposing the overall adversarial effects into elementary effects on different interactions.

- **We discover that adversarial perturbations mainly affect high-order interactions, rather than low-order interactions.** In comparison, low-order interactions are naturally robust to attacks. More specifically, the effects of adversarial perturbations on high-order interactions consist of three aspects: (1) High-order interactions *w.r.t.* the ground-truth category decrease significantly. (2) Interactions *w.r.t.* other labels usually increase a bit. (3) High-order interactions *w.r.t.* the target label increase the most.

We have proven that high-order interactions usually reflect complex pixel-wise mutual information under conditions of global collaborations. Low-order interactions usually represent simple pixel-wise mutual information *w.r.t.* simple and local collaborations. We further visualize interaction contexts of different orders, which also verify above findings. *In other words, adversarial attacks mainly affect complex features, which reflect complex collaborations between most pixels in the image.*

- A clear difference between standard DNNs and adversarially trained DNNs is as follows. **Adversarial training increases the robustness of high-order interactions, although high-order interactions are still more sensitive than low-order interactions.** In other words, compared with attacks towards standard DNNs, attacks towards adversarially trained DNNs are more likely to penalize both complex features of global (high-order) collaborations and simple features of local (low-order) collaborations, instead of exclusively punishing global collaborations.

- Then, we further explore the explanation for the high robustness of adversarially trained DNNs. **We find that the disentanglement of low-order interactions may account for this phenomenon.** We propose a disentanglement metric for interactions of a specific order. This metric examines whether or not the corresponding interactions represent discriminative information for a specific category. We discover that the disentanglement of low-order interactions learned by standard

DNNs are higher than those learned by adversarially trained DNNs. This indicates that adversarially trained DNNs encode more discriminative low-order interactions, than standard DNNs.

The disentanglement of low-order interactions makes the high-order interactions of adversarially trained DNNs robust to attacks. It is because features corresponding to high-order interactions are usually computed based on features of low-order interactions. The high disentanglement of low-order interactions makes it difficult to assemble low-order interactions of the ground-truth category into high-order features of an incorrect category. For example, in Figure 1, simple features (low-order interactions) are learned to represent the blue water and object parts, which are discriminative for the red-breasted merganser category. In this case, it is difficult to attack this image towards other categories, *e.g.* the bicycle category, because it is difficult to use the low-order blue water features to construct high-order bicycle features.

Above findings slightly revise the previous explanation of adversarially learned features in terms of shape-biased representations. Goodfellow et al. (2014); Tsipras et al. (2018); Dong et al. (2017); Zhang & Zhu (2019) claimed that adversarial training learned more interpretable representation features, which were usually biased to foreground shapes. We discover that these adversarially learned features are actually low-order interactions (local features), instead of modeling global foreground shapes.

- **Furthermore, the proposed interactions can be used (1) to explain the essential mechanism for the success of the attribution-based detection of adversarial examples (Yang et al., 2019); (2) to explain the recoverability of adversarial examples to normal samples; (3) to correct the network output on adversarial examples.**

Contributions of this paper can be summarized as follows. (1) We explain the difference between normal samples and adversarial examples *w.r.t.* ℓ_∞ attacks from a new perspective, *i.e.* the distinct signal-processing behavior of these adversarial examples. (2) We further explain the mechanism of how the adversarial training makes features robust to attacks, and explain the recoverability of adversarial examples to normal samples. (3) In order to explain adversarial training, we novelly define the multi-order interaction in game theory. The proposed interaction satisfies six properties, which demonstrate its rigorousness and solid theoretic foundation. (4) Our findings slightly revise the previous understanding of the shape bias of adversarially learned features. Furthermore, our finding can also explain the attribution-based method of detecting adversarial examples.

2. Related work

Adversarial attacks and defense. Attacking methods can be roughly summarized into white-box attacks (Szegedy et al., 2013; Goodfellow et al., 2014; Kurakin et al., 2016; Papernot et al., 2016a; Carlini & Wagner, 2017; Madry et al., 2018) and black-box attacks (Liu et al., 2016; Papernot et al., 2017; Chen et al., 2017; Bhagoji et al., 2018; Ilyas et al., 2018). For defense, adversarial training is one of the most widely-used defense method (Goodfellow et al., 2014; Kurakin et al., 2016; Papernot et al., 2016b; Tramèr et al., 2018). Other defense methods include masking gradients (Papernot et al., 2017; Nayebi & Ganguli, 2017), modifying networks (Cisse et al., 2017; Gao et al., 2017), and applying pre-processing on the input image for testing (Das et al., 2017; Meng & Chen, 2017; Xie et al., 2019).

Explanations for adversarial examples. Some previous studies focused on the reason for the existence of adversarial examples. Goodfellow et al. (2014) explained adversarial examples as a result of high linearity of feature representations. Gilmer et al. (2018) proved that the existence of adversarial examples was due to the geometry of the high-dimensional manifold. Xie et al. (2019); Xu et al. (2018; 2019) discovered that adversarial perturbations usually activated substantial “noise” and semantically irrelevant features. Engstrom et al. (2019) investigated the vulnerability of DNNs to rotations and translations. Tsipras et al. (2018); Ilyas et al. (2019) demonstrated that adversarial examples were attributed to non-robust yet discriminative features.

Understandings of adversarial training. Athalye et al. (2018) proved that adversarial training caused the obfuscated gradients phenomenon, which boosted the robustness. Goodfellow et al. (2014); Dong et al. (2017); Tsipras et al. (2018); Zhang & Zhu (2019) found that adversarially trained DNNs learned more shape-biased features than standard DNNs. Chalasani et al. (2020) proved that adversarially trained DNNs *w.r.t.* the ℓ_∞ attack exhibited more sparse attributions. Song et al. (2018) considered the adversarial training as the enumeration of all potential adversarial perturbations. Wang et al. (2019) explained adversarial training from the perspective of min-max optimization.

Understanding of the robustness. Szegedy et al. (2013); Hein & Andriushchenko (2017) computed Lipschitz constant to explain the robustness. Ignatiev et al. (2019); Boopathy et al. (2020) investigated the connection between network

interpretability and adversarial robustness. Tsipras et al. (2018) proved the inherent tension between adversarial robustness and standard generalization power. Fawzi et al. (2018); Gilmer et al. (2018); Weng et al. (2018) proved lower/upper bounds on the robustness.

Unlike previous explanations of adversarial attacks and defense, this paper explains adversarial examples and adversarial training from a new perspective, *i.e.* signal-processing behaviors of DNNs on adversarial examples.

Interactions. Interactions between input variables of a DNN have been widely investigated in recent years. In game theory, Grabisch & Roubens (1999); Lundberg et al. (2018) proposed and used the Shapley interaction index based on Shapley values (Shapley, 1953). Covert et al. (2020) investigated the relationship between the Shapley value and the mutual information. Sorokina et al. (2008) measured the interaction of multiple input variables in an additive model. Tsang et al. (2018) calculated interactions of weights in a DNN. Wang et al. (2021) applied the interaction of adversarial perturbations to understand adversarial transferability. Murdoch et al. (2018); Singh et al. (2018); Jin et al. (2019) used contextual decomposition (CD) technique to extract variable interactions. Cui et al. (2019) proposed a non-parametric probabilistic method to measure interactions using a Bayesian neural network. Janizek et al. (2020) extended the Integrated Gradients method (Sundararajan et al., 2017) to explain pairwise feature interactions in DNNs. Sundararajan et al. (2020) defined the Shapley-Taylor index to measure interactions over binary features. In comparison, we novelly define the multi-order interaction to understand the detailed interaction behaviors under different contextual complexities, which enable us to explain adversarial examples and adversarial training.

3. Interactions based on Shapley values

Preliminaries: Shapley values. The Shapley value (Shapley, 1953) in game theory is widely considered as an unbiased estimation for importance or contribution of each player in a game. Given the game with multiple players $N = \{1, 2, \dots, n\}$, some players cooperate to pursue a high reward to the game. Shapley values aim to fairly divide and assign the total reward to each individual player. In this way, the reward can be considered as the sum of elementary rewards of different players. Let $2^N \stackrel{\text{def}}{=} \{S | S \subseteq N\}$ denote all potential subsets of N . The game $v : 2^N \rightarrow \mathbb{R}$ is a function that estimates the overall reward $v(S)$ obtained by each specific subset of players $S \subseteq N$. In this way, the Shapley value $\phi(i|N)$ unbiasedly measures the elementary reward of the player i *w.r.t.* the total reward of all players.

$$\phi(i|N) = \sum_{S \subseteq N \setminus \{i\}} p(S) [v(S \cup \{i\}) - v(S)] \quad (1)$$

where $p(S) \stackrel{\text{def}}{=} \frac{(n-|S|-1)!|S|!}{n!}$. The Shapley value has been proved to satisfy four desirable properties, *i.e.* **linearity**, **nullity**, **symmetry** and **efficiency** properties, thereby being regarded as a fair method to allocate the total reward to each player (Weber, 1988). Please see the supplementary material for more details.

3.1. Definition of multi-order interactions

Using Shapley values to explain DNNs. Given a trained DNN and the input with n variables $N = \{1, \dots, n\}$, we can take the input variables as players, and consider the network output as the reward. The Shapley value $\phi(i|N)$ of each input variable $i \in N$ is regarded as the importance of the variable i to the network output. Each subset of variables $S \subseteq N$ represents a specific context. $v(S)$ represents the network output, when we keep variables in S unchanged and mask variables in $N \setminus S$ by following settings in (Ancona et al., 2019). In particular, $v(N)$ refers to the network output *w.r.t.* the entire input N , and $v(\emptyset)$ denotes the output when we mask all variables. Note that for the DNN trained for multi-category classification, $v(S)$ can be taken as an arbitrary dimension of the network output, so as to measure the variable importance to the corresponding category.

Shapley interaction index. Input variables of a DNN do not contribute to the network output independently. Instead, there are interactions/collaborations between different variables. To this end, the Shapley interaction index (Grabisch & Roubens, 1999) measures the influence of a variable on the Shapley value (importance) of another variable. *I.e.* for two variables (i, j) , it examines whether the absence/presence of j can change the importance of i . Thus, the Shapley interaction index is defined as the change in the Shapley value (importance) of variable i when the variable j is always present *w.r.t.* the case when j is always absent, as follows.

$$I(i, j) = \tilde{\phi}(i|N)_{j \text{ always present}} - \tilde{\phi}(i|N)_{j \text{ always absent}} \quad (2)$$

where $\tilde{\phi}(i|N)_{j \text{ always present}}$ denotes the Shapley value of the variable i computed under the specific condition that j is always

present. $\tilde{\phi}(i|N)_j$ always absent is computed under the specific condition that j is always absent. Note that $I(i, j) = I(j, i)$. Please see (Grabisch & Roubens, 1999) for more details about $I(i, j)$. If $I(i, j) > 0$, it indicates that the presence of the variable j will increase the importance of the variable i . Thus, we consider variables (i, j) have a positive interaction. If $I(i, j) < 0$, it indicates a negative interaction.

Multi-order interaction $I_{ij}^{(m)}$. In this paper, we further define interactions of different orders. We prove that the above Shapley interaction index $I(i, j)$ can be decomposed into interactions of different orders as follows (please see the proof in the supplementary material).

$$I(i, j) = \frac{1}{n-1} \sum_{m=0}^{n-2} I_{ij}^{(m)}, \quad I_{ij}^{(m)} = \mathbb{E}_{\substack{S \subseteq N \setminus \{i, j\} \\ |S|=m}} [\Delta v(i, j, S)] \quad (3)$$

where $\Delta v(i, j, S) \stackrel{\text{def}}{=} v(S \cup \{i, j\}) - v(S \cup \{i\}) - v(S \cup \{j\}) + v(S)$. $I_{ij}^{(m)}$ denotes the interaction of the m -th order, which measures the average interaction between variables (i, j) under all contexts consisting of m variables (e.g. visual contexts consisting of m pixels). For a low order m , $I_{ij}^{(m)}$ reflects the interaction between i and j w.r.t. simple contextual collaborations with a few variables. For a high order m , $I_{ij}^{(m)}$ corresponds to the interaction w.r.t. complex contextual collaborations with massive variables.

In this way, $I_{ij}^{(m)}$ encodes the additional importance scores brought by collaborations among (i, j) and other m variables. We have proven that $I_{ij}^{(m)}$ satisfies **linearity**, **nullity**, **commutativity**, **symmetry**, and **efficiency** properties (please see the supplementary material for details). In particular, we introduce the *efficiency property* here, which will be used for the explanation for adversarial training.

- **Efficiency property:** The output of the DNN can be decomposed into interactions of different orders, i.e. $v(N) = v(\emptyset) + \sum_{i \in N} \phi^{(0)}(i|N) + \sum_{i, j \in N, i \neq j} \sum_{m=0}^{n-2} J_{ij}^{(m)}$, where $J_{ij}^{(m)} \stackrel{\text{def}}{=} \frac{n-1-m}{n(n-1)} I_{ij}^{(m)}$, and $\phi^{(0)}(i|N) \stackrel{\text{def}}{=} v(i) - v(\emptyset)$.

3.2. Equivalence between the interaction and the mutual information

When a DNN outputs a probability distribution, we have proven that its interaction can be represented in the form of mutual information. Without loss of generality, let us take the image classification task for example. Let $x \in X \subseteq \mathbb{R}^n$ denote the input image of the DNN. x_i denotes the i -th pixel, and $X_i = \{x_i\}$. $\forall S \subseteq N$, we define $X_S = \{x_S | x \in X\}$; each x_S represents the image, where pixels in S remain unchanged, and other pixels $j \in N \setminus S$ are masked following settings of (Ancona et al., 2019). Let $y \in Y = \{y^1, \dots, y^C\}$ denote the network prediction. In this way, given x_S as the input, $p(y|x_S)$ denotes the output probability of the DNN. Let us set $v(S) = H(Y|X_S) = \sum_{x_S} p(x_S) H(Y|X_S = x_S)$, which measures the entropy of y given the input x_S . Then we have proven that

$$I_{ij}^{(m)} = \mathbb{E}_{\substack{S \subseteq N \setminus \{i, j\}, |S|=m}} MI(X_i; X_j; Y|X_S) \quad (4)$$

The conditional mutual information $MI(X_i; X_j; Y|X_S)$ measures the remaining mutual information between X_i , X_j and Y , when X_S is given. Note that unlike the bivariate mutual information, $MI(X_i; X_j; Y|X_S)$ can be negative. When X_S (with m pixels) is given, we can roughly understand the conditional mutual information $MI(X_{\{i, j\}}; Y|X_S)$ as the additional benefits from X_i and X_j to classification. We prove that $MI(X_{\{i, j\}}; Y|X_S)$ can be decomposed into the exclusive benefit of X_i , $MI(X_i; Y|X_j, X_S)$, the exclusive benefit of X_j , $MI(X_j; Y|X_i, X_S)$, and the benefit shared by X_i and X_j , i.e. $MI(X_i; X_j; Y|X_S)$. Thus, $MI(X_i; X_j; Y|X_S)$ can be considered as the benefit from the interaction between X_i and X_j . Please see the supplementary material for the proof.

4. Explaining adversarial attacks and defense using interactions

To simplify the story, we only study the simplest and widely-used untargeted and targeted ℓ_∞ PGD attacks (Madry et al., 2018). *Experiments based on other attacking methods (Dong et al., 2018) also verify our conclusions. Please see the supplementary material for details.*

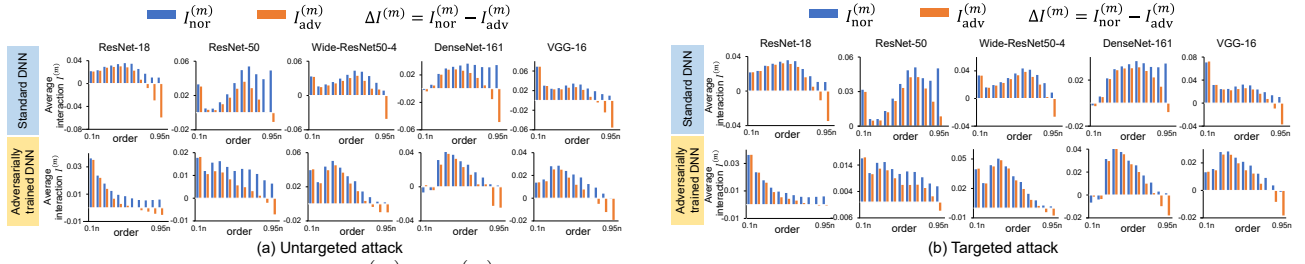


Figure 2. The multi-order interaction $I_{\text{nor}}^{(m)}$ and $I_{\text{adv}}^{(m)}$ of standard DNNs and adversarially trained DNNs. Adversarial perturbations mainly affected high-order interactions. **Results based on the Tiny-ImageNet dataset are shown in the supplementary material.**

4.1. Attacks mainly affect high-order interactions

Using the interaction defined above, we discover that adversarial perturbations mainly affect high-order interactions, rather than low-order interactions. In fact, according to the *efficiency property* of the interaction in Section 3.1, the output of the DNN *w.r.t.* the image x can be decomposed into the sum of multi-order interactions between different pairs of input variables. Thus, we can decompose the overall effects of adversarial perturbations on the network output into elementary effects on interactions, as follows.

$$\Delta v(N|x) \stackrel{\text{def}}{=} v(N|x) - v(N|\tilde{x}) = \Delta v(\emptyset|x) + \underbrace{\sum_{i \in N} \Delta \phi^{(0)}(i|N, x)}_{\text{usually can be ignored}} + \sum_{i \neq j \in N} \sum_{m=0}^{n-2} \Delta J_{ij}^{(m)}(x) \quad (5)$$

where $x \in \mathbb{R}^n$ denotes the normal sample, and $\tilde{x} = x + \Delta x \in \mathbb{R}^n$ denotes the adversarial example. $v(N|\tilde{x})$ denotes the network output given all variables in N of the adversarial example \tilde{x} . $v(N|x)$ corresponds to the normal sample. The first term $\Delta v(\emptyset) = v(\emptyset|x) - v(\emptyset|\tilde{x}) = 0$. In the second term, $\Delta \phi^{(0)}(i|N, x) \stackrel{\text{def}}{=} (v(i|x) - v(\emptyset|x)) - (v(i|\tilde{x}) - v(\emptyset|\tilde{x})) = v(i|x) - v(i|\tilde{x})$. Because in most applications, the importance of a single variable (*e.g.* a pixel) is usually small, we can ignore this term. In the third term, $\Delta J_{ij}^{(m)}(x)$ denotes the attacking utility of the m -order interaction between variables (i, j) in x . $\Delta J_{ij}^{(m)}(x) \stackrel{\text{def}}{=} \frac{n-1-m}{n(n-1)} \Delta I_{ij}^{(m)}(x)$, where $\Delta I_{ij}^{(m)}(x) \stackrel{\text{def}}{=} I_{ij}^{(m)}(x) - I_{ij}^{(m)}(\tilde{x})$ measures the elementary effects of adversarial perturbations on the m -order interaction. $I_{ij}^{(m)}(x)$ and $I_{ij}^{(m)}(\tilde{x})$ denote the m -order interactions in the normal sample x and that in the adversarial example \tilde{x} , respectively.

Therefore, according to the above equation, effects of adversarial attacks mainly depend on changes of interactions $\Delta I_{ij}^{(m)}(x)$ (or $\Delta J_{ij}^{(m)}(x)$). Thus, in this section, we further conduct experiments to show that adversarial attacks mainly affect $\Delta I_{ij}^{(m)}(x)$ of high orders.

Metric. We compute the average interaction of a specific order m among different pairs of variables in different input images, *i.e.* $I^{(m)} = \mathbb{E}_{x \in \Omega} \mathbb{E}_{i,j} [I_{ij}^{(m)}(x)]$, where $\Omega \subseteq \mathbb{R}^n$ denotes the set of all samples. We can use the set of normal samples Ω_{nor} to compute $I_{\text{nor}}^{(m)}$ and use the set of adversarial examples Ω_{adv} to compute $I_{\text{adv}}^{(m)}$. In this way, $\Delta I^{(m)} \stackrel{\text{def}}{=} I_{\text{nor}}^{(m)} - I_{\text{adv}}^{(m)}$ measures the difference in interactions between normal samples and adversarial examples. We further prove that $\Delta I^{(m)} = \mathbb{E}_{x \in \Omega} \mathbb{E}_{i,j} [\Delta I_{ij}^{(m)}(x)]$. Thus, $\Delta I^{(m)}$ represents effects of attacks on the m -order interactions. Similarly, $\Delta J^{(m)} \stackrel{\text{def}}{=} \mathbb{E}_{x \in \Omega} \mathbb{E}_{i,j} [\Delta J_{ij}^{(m)}(x)] = \frac{n-1-m}{n(n-1)} \Delta I^{(m)}$. $\Delta J^{(m)}$ is a component of $\mathbb{E}_x (\Delta v(N|x))$ according to Eq. (5) (proof in the supplementary material).

Details of experimental settings. In order to measure $I_{\text{nor}}^{(m)}$ and $I_{\text{adv}}^{(m)}$, we conducted experiments on ResNet-18/34/50 (He et al., 2016), Wide-ResNet50-4 (Zagoruyko & Komodakis, 2016), DenseNet-161 (Huang et al., 2017), and VGG-16 (Simonyan & Zisserman, 2015). For each DNN, we obtained both the standard trained version and the adversarially trained version on the ImageNet dataset (Russakovsky et al., 2015)¹ or the Tiny-ImageNet dataset (Le & Yang, 2015). We measured the interaction $I^{(m)}$ by setting $v(S|x) = \log p(y = y^{\text{truth}}|S, x)$, where $x \in \Omega$ was sampled from the validation set. However, the computational cost of $I^{(m)}$ was intolerable. To reduce the computational cost, we did not compute interactions at the pixel-wise level. Instead, we split the image into 16×16 grids, and took each grid as a single input variable, thereby $n = 256$.

¹We used pretrained models released by Salman et al. (2020).

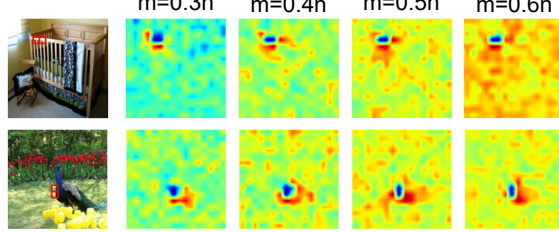


Figure 3. Contexts of the m -order interaction $I_{ij}^{(m)}$ in normal samples of standard ResNet-18. Variables (i, j) are indicated by red boxes. Low-order interactions usually reflected simple features with local collaborations, and high-order interactions usually represented complex features with global collaborations. **Results based on the standardly trained ResNet-50 are shown in the supplementary material.**

We considered both untargeted and targeted² PGD attacks (Madry et al., 2018) with the ℓ_∞ constraint $\|\Delta x\|_{\ell_\infty} \leq \epsilon$ to generate adversarial examples. We set $\epsilon = 32/255$ by following the setting in (Xie et al., 2019). The step size was set to $2/255$. For fair comparisons, we controlled the perturbation generated for each image to have similar attacking utility of 8. The attacking utility in untargeted attacks was defined as $U_{\text{untarget}}(x) = h_{y^{\text{truth}}}(N|x) - h_{y^{\text{truth}}}(N|\tilde{x})$, where $h_{y^{\text{truth}}}(N|x)$ and $h_{y^{\text{truth}}}(N|\tilde{x})$ denote network outputs of the ground-truth category y^{truth} before the softmax layer, when taking the normal sample and the adversarial example as input, respectively. The attacking utility in targeted attacks was defined as $U_{\text{target}}(x) = (h_{y^{\text{target}}}(N|\tilde{x}) - h_{y^{\text{truth}}}(N|\tilde{x})) - (h_{y^{\text{target}}}(N|x) - h_{y^{\text{truth}}}(N|x))$, where $h_{y^{\text{target}}}(\cdot)$ denote the network output of the target category² y^{target} .

Results. Figure 2 shows $I_{\text{nor}}^{(m)}$ and $I_{\text{adv}}^{(m)}$ of different orders *w.r.t.* the ground-truth category. We found that adversarial perturbations significantly decreased high-order interactions, in both adversarially trained DNNs and standard DNNs. For example, in Figure 2 (a), low-order interactions ($m < 0.5n$) in standard ResNet-18 decreased a little, while the interaction of order $m = 0.95n$ dropped from 0.01 to -0.059 . This phenomenon was consistent with the heuristic findings of Dong et al. (2017) that neurons corresponding to high-level semantics were ambiguous.

Additional experiments on the target category and other categories. Beyond above analysis about interactions *w.r.t.* the ground-truth category, we also conducted experiments and found that high-order interactions *w.r.t.* the target category² increased significantly. Please see the supplementary material for details. In sum, high-order interactions were much more sensitive than low-order interactions, which verified our conclusions.

Visualization of interaction contexts. Zhang et al. (2021c) proposed a method to visualize salient contexts $\{S\}$ of the Shapley interaction index $I(i, j)$ for each pair (i, j) . We extend this method to visualize the multi-order interaction $I_{ij}^{(m)}$ by exclusively considering contexts of a specific order. Results are shown in Figure 3. We found that high-order interactions usually reflected complex features with global collaborations, and low-order interactions usually represented simple features with local collaborations. Please see the supplementary material for more visualization results.

4.2. Explaining the attribution-based method of detecting adversarial examples

We propose the multi-order Shapley value $\phi^{(m)}(i|N, x) \stackrel{\text{def}}{=} \mathbb{E}_{S \subseteq N \setminus \{i\}, |S|=m} [v(S \cup i|x) - v(S|x)]$. We also prove that $\phi^{(m)}(i|N, x)$ can be decomposed into interactions of different orders, as follows.

$$v(N|x) - v(\emptyset|x) = \frac{1}{n} \sum_{i \in N} \sum_{m=0}^{n-1} \phi^{(m)}(i|N, x) \quad \phi^{(m)}(i|N, x) = \mathbb{E}_{j \in N \setminus \{i\}} \left[\sum_{k=0}^{m-1} I_{ij}^{(k)}(x) \right] + \phi^{(0)}(i|N, x) \quad (6)$$

where $\phi^{(0)}(i|N, x) = v(i|x) - v(\emptyset|x)$ is usually small and can be ignored, as discussed in texts below Eq. (5).

Yang et al. (2019) proposed an attribution-based method to detect adversarial examples, which used the attribution score of input variables. We have proven that the attribution score can be written as $\phi^{(n-1)}(i|N, x) = v(N|x) - v(N \setminus \{i\}|x)$. According to Eq. (6), the adversarial effects on the network output can also be decomposed into elementary effects on $\phi^{(m)}(i|N, x)$. Among all Shapley values of different orders m , only $\phi^{(n-1)}(i|N, x)$ contains the interactions of the highest order, *i.e.* the $(n-2)$ -order interactions, which are the most sensitive interactions to attacks, according to Section 4.1. Thus, $\phi^{(n-1)}(i|N, x)$ in normal samples and that in adversarial examples are supposed to exhibit significant difference, which enables the detection of adversarial examples. Please see the supplementary material for the detailed proof.

²In the untargeted attack, we considered the misclassified category as the target category. In the targeted attack, the target label was set as the misclassified category in the untarget attack.

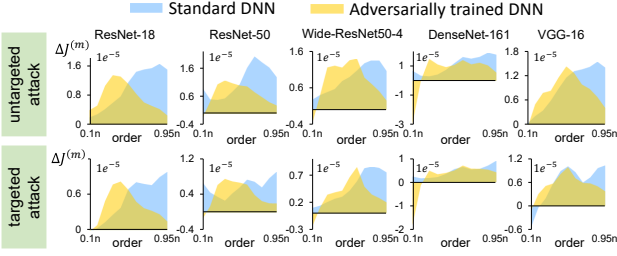


Figure 4. Distribution of compositional attacking utilities caused by interactions of different orders $\{\Delta J^{(m)}\}$, where $\Delta J^{(m)} = \frac{n-1-m}{n(n-1)} \Delta I^{(m)}$. For standard DNNs, attacks mainly affected high-order interactions. However, for adversarially trained DNNs, low-order interactions also had considerable attacking utility. **Results based on the Tiny-ImageNet dataset are shown in the supplementary material.**

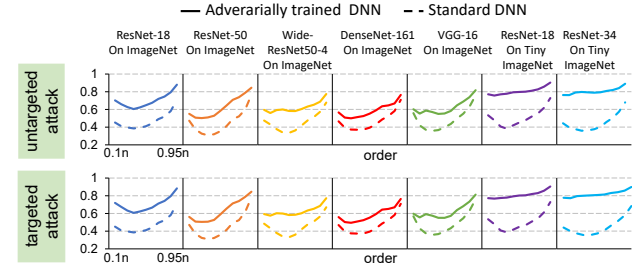


Figure 5. The interaction disentanglement $D^{(m)}$. Interactions of adversarially trained DNNs exhibited higher disentanglement than those of standard DNNs.

4.3. Explaining specific signal-processing behaviors of adversarially trained DNNs

Discovery. In order to understand the difference in signal-processing behaviors between adversarially trained DNNs and standard DNNs, we have proven that the overall attacking utility $\mathbb{E}_{x \in \Omega} [\Delta v(N|x)]$ can be approximately decomposed as the sum of $\Delta J^{(m)}$ of different orders $m = 0, 1, \dots, n-2$, according to Eq. (5). Figure 4 shows the attacking utility of multi-order interactions *i.e.* $\Delta J^{(m)} = \frac{n-1-m}{n(n-1)} \Delta I^{(m)}$.

We noticed that for standard DNNs, adversarial attacks mainly affected high-order interactions. For adversarially trained DNNs, although high-order interactions were usually sensitive to attacks, low/middle-order interactions took up more attacking utility. Considering Eq. (5), this indicated that adversarial perturbations towards adversarially trained DNNs penalized both complex features of global collaborations and simple features of local collaborations.

Explanation. We further explain the above phenomena, *i.e.* why high-order interactions in adversarially trained DNNs are more robust to attacks than those in standard DNNs. To this end, we propose the following disentanglement metric for the interaction of a specific order.

$$\begin{aligned} D^{(m)} &= \mathbb{E}_{x \in \Omega} \mathbb{E}_{i,j \in N} \frac{|I_{ij}^{(m)}(x)|}{\sum_{\substack{S \subseteq N \setminus \{i,j\}, |S|=m}} |\Delta v(i, j, S|x)|} \\ &= \mathbb{E}_{x \in \Omega} \mathbb{E}_{i,j \in N} \frac{|\sum_{\substack{S \subseteq N \setminus \{i,j\}, |S|=m}} \Delta v(i, j, S|x)|}{\sum_{\substack{S \subseteq N \setminus \{i,j\}, |S|=m}} |\Delta v(i, j, S|x)|} \end{aligned} \quad (7)$$

The above disentanglement metric examines whether or not the m -order interactions represent discriminative information for a specific category. The high value of $D^{(m)}$ indicates that the m -order interactions relatively purify describe specific categories. In other words, the interactions between (i, j) under different contexts S consistently have the same effects (either positive or negative) on the inference of a specific category. Let us consider the following toy example. When the pair of (i, j) consistently have positive interactions towards a specific category under different contexts, *i.e.* $\forall S \subseteq N \setminus \{i, j\}, |S|=m, \Delta v(i, j, S|x) > 0$, then we have $D^{(m)} = 1$. This means that the m -th interactions between i and j stably promote the output probability of this category. In contrast, a low value of $D^{(m)}$ indicates that interactions between (i, j) represent diverse categories. *I.e.* given different contexts S , interactions between (i, j) sometimes have positive effects on a specific category, and sometimes have negative effects.

Experiments. Figure 5 compares the interaction disentanglement $D^{(m)}$ of standard DNNs and the disentanglement of adversarially trained DNNs. Interactions of adversarially trained DNNs were more disentangled than those of standard DNNs, especially for low-order interactions. This indicated that low-order interactions in adversarially trained DNNs encoded more category-specific information for inference than low-order interactions in standard DNNs.

Based on this observation, we could explain the robustness of high-order interactions to attacks in adversarially trained DNNs. Adversarial training learned more category-specific low-order interactions, which boosted the difficulty of attacking high-order interactions. This was because that high-order interactions (usually global features) were usually constructed by low-order interactions (usually local features). Let us take the peacock in Figure 3 for example. In this image, low-order interactions (simple features) represented the body of the peacock and the green garden. In this case, it was difficult to attack this image to other categories (*e.g.* the bicycle category) by constructing high-order interactions of the bicycle category

Table 1. The distance between normal samples x and adversarial examples \tilde{x} , and the distance between x and the recovered samples \hat{x} . For adversarially trained DNNs, the recovered samples were more close to normal samples than adversarial examples. For standard DNNs, the recovered samples were farther from normal samples than adversarial examples.

	Standard DNN		Adversarially trained DNN	
	$\mathbb{E}\ x - \tilde{x}\ _2$	$\mathbb{E}\ x - \hat{x}\ _2$	$\mathbb{E}\ x - \tilde{x}\ _2$	$\mathbb{E}\ x - \hat{x}\ _2$
ResNet-18	9.72	13.57	18.69	11.45
ResNet-50	9.56	13.40	18.34	12.68
DenseNet-161	9.67	13.51	18.55	13.26

Table 2. Ratio of adversarial examples whose classification results were corrected. Our method corrected the classification of more adversarial examples than the cutout method.

Standard DNNs	cutout	ours			Adversarially trained DNNs	cutout	ours		
		$\alpha = 0.1$	$\alpha = 0.2$	$\alpha = 0.3$			$\alpha = 0.1$	$\alpha = 0.2$	$\alpha = 0.3$
ResNet-18	7.12%	19.62%	35.55%	44.14%	ResNet-18	23.92%	22.46%	33.78%	39.18%
ResNet-50	10.63%	28.53%	45.53%	52.33%	ResNet-50	24.27%	23.23%	35.23%	41.54%
DenseNet-161	11.32%	27.16%	46.15%	56.35%	DenseNet-161	35.65%	24.65%	39.25%	45.74%

using these peacock low-order features. Due to the difficulty of attacking high-order interactions, the adversarially trained DNN had to attack low-order interactions, instead.

4.4. Explaining recoverability of adversarial examples

In this section, we aim to use the multi-order interaction to explain the capacity of recovering adversarial examples to normal samples. The adversarial recoverability of a DNN is referred to as whether the DNN’s adversarial examples can be inverted back to the normal sample by minimizing the classification loss. Specifically, let the untargeted attack (Madry et al., 2018) minimize the classification loss of the normal sample x , and generate the adversarial example \tilde{x} . Then, we conduct a targeted attack (Madry et al., 2018) on the adversarial sample \tilde{x} , which inverts the classification result back to its ground-truth label. Let \hat{x} denote the sample recovered from \tilde{x} . If the recovered sample \hat{x} is more close to x than \tilde{x} using the Euclidean distance, it indicates a high recoverability; otherwise, a low recoverability.

Experiments. Based on ResNet-18/50 and DenseNet-161 trained on the ImageNet dataset, we generated adversarial examples for normal validation samples in the ImageNet dataset, using the ℓ_∞ untargeted PGD attack ($\epsilon = 16/255$). The attack was conducted with 10 steps with the step size 2/255. Then, we used same parameters to conduct the targeted PGD attack and recover normal examples.

Table 1 shows that adversarially trained DNNs usually exhibited higher recoverability than standard DNNs. This can be explained by Eq. (14). As we have discussed in Section 4.3, adversarial perturbations towards adversarially trained DNNs usually pay more attention to low-order interactions than perturbations towards standard DNNs. On the other hand, the low-order interaction $I_{ij}^{(m)}(x)$ is equivalent to the conditional mutual information $MI(X_i; X_j; Y|X_S)$ given small contexts X_S according to Eq. (14), while the high-order interaction corresponds to such a mutual information conditioned on large contexts with massive variables. In general, compared to high-order interactions, low-order interactions are conditioned on less contextual variables, thereby suffering less from adversarial perturbations, *i.e.* obviously $MI(X_i; X_j; Y|X_S)$ usually suffers less from adversarial perturbations, if the condition x_S only contains very few variables. In other words, low-order interactions are more transferable among different contexts x_S , so it is easy to invert adversarial perturbations of low-order interactions. In this way, because adversarial perturbations for adversarially trained DNNs mainly focus on low-order interactions, such perturbations are easy to be recovered.

Note that in Eq. (14), we set $\hat{v}(S) = H(Y|X_S)$, which is slightly different from setting $v(S) = \log p(y = y^{\text{truth}}|S, x)$ in Section 4.3. Nevertheless, the trend of $v(S)$ can roughly reflect the negative trend of $\hat{v}(S)$. Crucially, we also measured the change of multi-order interaction strength using $\hat{v}(S)$. We obtained the same conclusion, *i.e.* high-order interactions in adversarially trained DNNs were more robust than those in standard DNNs. Please see the supplementary material for details.

4.5. Correcting network outputs on adversarial examples

Based on the observation that adversarial attacks mainly affect high-order interactions, we try to reduce the attacking effects on the network output by removing these sensitive high-order interactions in adversarial examples. The removing

of high-order interactions may correct the network output on adversarial examples in the inference phase. Specifically, in experiments, we simply applied the dropout operation on the input sample, which mainly removed high-order interactions according to (Zhang et al., 2021b). This idea was similar to the cutout method (DeVries & Taylor, 2017), which randomly masked out a square region of the input during training and testing. Thus, we took the cutout method as a baseline.

Based on ResNet-18/50 and DenseNet-161 trained on the ImageNet dataset, we used the correctly classified normal samples in the validation set of the ImageNet dataset, and generated adversarial examples with the ℓ_∞ untarget PGD attack following settings in (Xie et al., 2019), and the attack was stopped once it succeeded. We applied the dropout operation with different rates α at the pixel-level, and the dropped pixels were filled with the average value of surrounding pixels. For the cutout method, we set the length of the side of the masked square regions as 112, which was half of the side length of the input sample (dropping $\alpha = 25\%$ pixels of the input), following settings in (DeVries & Taylor, 2017).

Table 2 reports the ratio of adversarial examples whose classification results were corrected. When we applied dropout to adversarial examples, the classification accuracy of adversarial examples significantly increased, and performed better than the baseline method. We have also theoretically proved the effectiveness of this method. Please see the supplementary material for the proof.

5. Conclusion

In this paper, we have proposed the multi-order interaction to provide a unified understanding of signal-processing behaviors in adversarial attacks and defense. Based on the multi-order interaction, we have discovered that adversarial attacks mainly affected high-order interactions. Meanwhile, we have also found that adversarial training actually learned more category-specific low-order interactions to boost the robustness. Besides above explanations, we also used the multi-order interactions to explain the attribution-based method of detecting adversarial examples, and explain the recoverability of adversarial examples.

References

Ancona, M., Oztireli, C., and Gross, M. Explaining deep neural networks with a polynomial time algorithm for shapley value approximation. In *International Conference on Machine Learning*, pp. 272–281. PMLR, 2019.

Athalye, A., Carlini, N., and Wagner, D. Obfuscated gradients give a false sense of security: Circumventing defenses to adversarial examples. In *International Conference on Machine Learning*, pp. 274–283, 2018.

Bhagoji, A. N., He, W., Li, B., and Song, D. Practical black-box attacks on deep neural networks using efficient query mechanisms. In *European Conference on Computer Vision*, pp. 158–174. Springer, 2018.

Boopathy, A., Liu, S., Zhang, G., Liu, C., Chen, P.-Y., Chang, S., and Daniel, L. Proper network interpretability helps adversarial robustness in classification. In *International Conference on Machine Learning*, pp. 1014–1023. PMLR, 2020.

Carlini, N. and Wagner, D. Towards evaluating the robustness of neural networks. In *2017 ieee symposium on security and privacy (sp)*, pp. 39–57. IEEE, 2017.

Chalasani, P., Chen, J., Chowdhury, A. R., Wu, X., and Jha, S. Concise explanations of neural networks using adversarial training. In *International Conference on Machine Learning*, pp. 1383–1391. PMLR, 2020.

Chen, P.-Y., Zhang, H., Sharma, Y., Yi, J., and Hsieh, C.-J. Zoo: Zeroth order optimization based black-box attacks to deep neural networks without training substitute models. In *Proceedings of the 10th ACM Workshop on Artificial Intelligence and Security*, pp. 15–26, 2017.

Cisse, M., Adi, Y., Neverova, N., and Keshet, J. Houdini: Fooling deep structured prediction models. *arXiv preprint arXiv:1707.05373*, 2017.

Covert, I., Lundberg, S., and Lee, S.-I. Understanding global feature contributions with additive importance measures. *Advances in Neural Information Processing Systems*, 33, 2020.

Cui, T., Marttinen, P., and Kaski, S. Learning global pairwise interactions with bayesian neural networks. *arXiv preprint arXiv:1901.08361*, 2019.

Das, N., Shanbhogue, M., Chen, S.-T., Hohman, F., Chen, L., Kounavis, M. E., and Chau, D. H. Keeping the bad guys out: Protecting and vaccinating deep learning with jpeg compression. *arXiv preprint arXiv:1705.02900*, 2017.

DeVries, T. and Taylor, G. W. Improved regularization of convolutional neural networks with cutout. *arXiv preprint arXiv:1708.04552*, 2017.

Dong, Y., Su, H., Zhu, J., and Bao, F. Towards interpretable deep neural networks by leveraging adversarial examples. *arXiv preprint arXiv:1708.05493*, 2017.

Dong, Y., Liao, F., Pang, T., Su, H., Zhu, J., Hu, X., and Li, J. Boosting adversarial attacks with momentum. In *Proceedings of the IEEE conference on computer vision and pattern recognition*, pp. 9185–9193, 2018.

Engstrom, L., Tran, B., Tsipras, D., Schmidt, L., and Madry, A. Exploring the landscape of spatial robustness. In *International Conference on Machine Learning*, pp. 1802–1811. PMLR, 2019.

Fawzi, A., Fawzi, O., and Frossard, P. Analysis of classifiers’ robustness to adversarial perturbations. *Machine Learning*, 107(3):481–508, 2018.

Gao, J., Wang, B., Lin, Z., Xu, W., and Qi, Y. Deepcloak: Masking deep neural network models for robustness against adversarial samples. *arXiv preprint arXiv:1702.06763*, 2017.

Gilmer, J., Metz, L., Faghri, F., Schoenholz, S. S., Raghu, M., Wattenberg, M., Goodfellow, I., and Brain, G. The relationship between high-dimensional geometry and adversarial examples. *arXiv preprint arXiv:1801.02774*, 2018.

Goodfellow, I. J., Shlens, J., and Szegedy, C. Explaining and harnessing adversarial examples. *arXiv preprint arXiv:1412.6572*, 2014.

Grabisch, M. and Roubens, M. An axiomatic approach to the concept of interaction among players in cooperative games. *International Journal of game theory*, 28(4):547–565, 1999.

He, K., Zhang, X., Ren, S., and Sun, J. Deep residual learning for image recognition. In *CVPR*, 2016.

Hein, M. and Andriushchenko, M. Formal guarantees on the robustness of a classifier against adversarial manipulation. In *Advances in neural information processing systems*, pp. 2266–2276, 2017.

Huang, G., Liu, Z., Van Der Maaten, L., and Weinberger, K. Q. Densely connected convolutional networks. In *Proceedings of the IEEE conference on computer vision and pattern recognition*, pp. 4700–4708, 2017.

Ignatiev, A., Narodytska, N., and Marques-Silva, J. On relating explanations and adversarial examples. In *Advances in Neural Information Processing Systems*, pp. 15883–15893, 2019.

Ilyas, A., Engstrom, L., Athalye, A., and Lin, J. Black-box adversarial attacks with limited queries and information. In *International Conference on Machine Learning*, pp. 2137–2146, 2018.

Ilyas, A., Santurkar, S., Tsipras, D., Engstrom, L., Tran, B., and Madry, A. Adversarial examples are not bugs, they are features. In *Advances in Neural Information Processing Systems*, pp. 125–136, 2019.

Janizek, J. D., Sturmels, P., and Lee, S.-I. Explaining explanations: Axiomatic feature interactions for deep networks. *arXiv preprint arXiv:2002.04138*, 2020.

Jin, X., Wei, Z., Du, J., Xue, X., and Ren, X. Towards hierarchical importance attribution: Explaining compositional semantics for neural sequence models. In *International Conference on Learning Representations*, 2019.

Kurakin, A., Goodfellow, I., and Bengio, S. Adversarial examples in the physical world. *arXiv preprint arXiv:1607.02533*, 2016.

Le, Y. and Yang, X. Tiny imagenet visual recognition challenge. *CS 231N*, 7, 2015.

Liu, Y., Chen, X., Liu, C., and Song, D. Delving into transferable adversarial examples and black-box attacks. 2016.

Lundberg, S. M., Erion, G. G., and Lee, S.-I. Consistent individualized feature attribution for tree ensembles. *arXiv preprint arXiv:1802.03888*, 2018.

Madry, A., Makelov, A., Schmidt, L., Tsipras, D., and Vladu, A. Towards deep learning models resistant to adversarial attacks. In *International Conference on Learning Representations*, 2018.

Meng, D. and Chen, H. Magnet: a two-pronged defense against adversarial examples. In *Proceedings of the 2017 ACM SIGSAC conference on computer and communications security*, pp. 135–147, 2017.

Murdoch, W. J., Liu, P. J., and Yu, B. Beyond word importance: Contextual decomposition to extract interactions from lstms. In *International Conference on Learning Representations*, 2018.

Nayebi, A. and Ganguli, S. Biologically inspired protection of deep networks from adversarial attacks. *arXiv preprint arXiv:1703.09202*, 2017.

Papernot, N., McDaniel, P., Jha, S., Fredrikson, M., Celik, Z. B., and Swami, A. The limitations of deep learning in adversarial settings. In *2016 IEEE European symposium on security and privacy (EuroS&P)*, pp. 372–387. IEEE, 2016a.

Papernot, N., McDaniel, P., Wu, X., Jha, S., and Swami, A. Distillation as a defense to adversarial perturbations against deep neural networks. In *2016 IEEE Symposium on Security and Privacy (SP)*, pp. 582–597. IEEE, 2016b.

Papernot, N., McDaniel, P., Goodfellow, I., Jha, S., Celik, Z. B., and Swami, A. Practical black-box attacks against machine learning. In *Proceedings of the 2017 ACM on Asia conference on computer and communications security*, pp. 506–519, 2017.

Russakovsky, O., Deng, J., Su, H., Krause, J., Satheesh, S., Ma, S., Huang, Z., Karpathy, A., Khosla, A., Bernstein, M., Berg, A. C., and Fei-Fei, L. Imagenet large scale visual recognition challenge. In *International Journal of Computer Vision*, 115(3):211–252, 2015.

Salman, H., Ilyas, A., Engstrom, L., Kapoor, A., and Madry, A. Do adversarially robust imagenet models transfer better? *arXiv preprint arXiv:2007.08489*, 2020.

Shapley, L. S. A value for n-person games. *Contributions to the Theory of Games*, 2(28):307–317, 1953.

Simonyan, K. and Zisserman, A. Very deep convolutional networks for large-scale image recognition. In *ICLR*, 2015.

Singh, C., Murdoch, W. J., and Yu, B. Hierarchical interpretations for neural network predictions. In *International Conference on Learning Representations*, 2018.

Song, Y., Shu, R., Kushman, N., and Ermon, S. Constructing unrestricted adversarial examples with generative models. *Advances in Neural Information Processing Systems*, 31:8312–8323, 2018.

Sorokina, D., Caruana, R., Riedewald, M., and Fink, D. Detecting statistical interactions with additive groves of trees. In *Proceedings of the 25th international conference on Machine learning*, pp. 1000–1007, 2008.

Sundararajan, M., Taly, A., and Yan, Q. Axiomatic attribution for deep networks. In *Proceedings of the 34th International Conference on Machine Learning-Volume 70*, pp. 3319–3328, 2017.

Sundararajan, M., Dhamdhere, K., and Agarwal, A. The shapley taylor interaction index. In *International Conference on Machine Learning*, pp. 9259–9268. PMLR, 2020.

Szegedy, C., Zaremba, W., Sutskever, I., Bruna, J., Erhan, D., Goodfellow, I., and Fergus, R. Intriguing properties of neural networks. *arXiv preprint arXiv:1312.6199*, 2013.

Tramèr, F., Kurakin, A., Papernot, N., Goodfellow, I., Boneh, D., and McDaniel, P. D. Ensemble adversarial training: Attacks and defenses. In *6th International Conference on Learning Representations, ICLR 2018*, 2018.

Tsang, M., Cheng, D., and Liu, Y. Detecting statistical interactions from neural network weights. In *International Conference on Learning Representations*, 2018.

Tsipras, D., Santurkar, S., Engstrom, L., Turner, A., and Madry, A. Robustness may be at odds with accuracy. In *International Conference on Learning Representations*, 2018.

Wang, X., Ren, J., Lin, S., Zhu, X., Wang, Y., and Zhang, Q. A unified approach to interpreting and boosting adversarial transferability. In *ICLR*, 2021.

Wang, Y., Ma, X., Bailey, J., Yi, J., Zhou, B., and Gu, Q. On the convergence and robustness of adversarial training. In *ICML*, volume 1, pp. 2, 2019.

Weber, R. J. Probabilistic values for games. *The Shapley Value. Essays in Honor of Lloyd S. Shapley*, pp. 101–119, 1988.

Weng, T.-W., Zhang, H., Chen, P.-Y., Yi, J., Su, D., Gao, Y., Hsieh, C.-J., and Daniel, L. Evaluating the robustness of neural networks: An extreme value theory approach. In *International Conference on Learning Representations*, 2018.

Xie, C., Wu, Y., Maaten, L. v. d., Yuille, A. L., and He, K. Feature denoising for improving adversarial robustness. In *Proceedings of the IEEE Conference on Computer Vision and Pattern Recognition*, pp. 501–509, 2019.

Xu, K., Liu, S., Zhao, P., Chen, P.-Y., Zhang, H., Fan, Q., Erdogmus, D., Wang, Y., and Lin, X. Structured adversarial attack: Towards general implementation and better interpretability. In *International Conference on Learning Representations*, 2018.

Xu, K., Liu, S., Zhang, G., Sun, M., Zhao, P., Fan, Q., Gan, C., and Lin, X. Interpreting adversarial examples by activation promotion and suppression. *arXiv preprint arXiv:1904.02057*, 2019.

Yang, P., Chen, J., Hsieh, C., Wang, J., and Jordan, M. I. ML-LOO: detecting adversarial examples with feature attribution. *CoRR*, abs/1906.03499, 2019. URL <http://arxiv.org/abs/1906.03499>.

Zagoruyko, S. and Komodakis, N. Wide residual networks. *arXiv preprint arXiv:1605.07146*, 2016.

Zhang, D., Zhou, H., Zhang, H., Bao, X., Huo, D., Chen, R., Cheng, X., Wu, M., and Zhang, Q. Building interpretable interaction trees for deep nlp models. In *AAAI*, 2021a.

Zhang, H., Cheng, X., Chen, Y., and Zhang, Q. Game-theoretic interactions of different orders. *arXiv preprint arXiv:2010.14978*, 2020.

Zhang, H., Li, S., Ma, Y., Li, M., Xie, Y., and Zhang, Q. Interpreting and boosting dropout from a game-theoretic view. In *ICLR*, 2021b.

Zhang, H., Xie, Y., Zheng, L., Zhang, D., and Zhang, Q. Interpreting multivariate interactions in dnns. In *AAAI*, 2021c.

Zhang, T. and Zhu, Z. Interpreting adversarially trained convolutional neural networks. In *International Conference on Machine Learning*, pp. 7502–7511, 2019.

A. Preliminaries: Shapley values

Given a complex system, the Shapley value is defined in game theory by [Shapley \(1953\)](#), and is widely considered as an unbiased estimation of the numerical importance *w.r.t.* each input variable. In game theory, the complex system is usually represented as a game, where each input variable is taken as a player, and the output of this system is regarded as the total reward of all players. Given a game with multiple players (input variables) $N = \{1, 2, \dots, n\}$, some players cooperate to pursue a high reward. Thus, the task is to divide the total reward, and fairly assign the divided elementary reward to each individual player. In this way, the elementary reward can be considered as the numerical importance of the corresponding variable to the complex system. Let $2^N \stackrel{\text{def}}{=} \{S | S \subseteq N\}$ indicate all potential subsets of N . The game $v : 2^N \rightarrow \mathbb{R}$ is a function, which estimates the overall reward $v(S)$ earned by each specific subset of players $S \subseteq N$. In this way, the Shapley value, denoted by $\phi(i|N)$, represents the numerical importance of the player i to the game v .

$$\phi(i|N) = \sum_{S \subseteq N \setminus \{i\}} \frac{(n - |S| - 1)! |S|!}{n!} [v(S \cup \{i\}) - v(S)]. \quad (8)$$

[Weber \(1988\)](#) has proven that the Shapley value is a unique method to fairly allocate overall reward to each player that satisfies following properties.

- (1) **Linearity property:** If two independent games can be merged into one game $u(S) = v(S) + w(S)$, then the Shapley value of the new game also can be merged, *i.e.* $\forall i \in N, \phi_u(i|N) = \phi_v(i|N) + \phi_w(i|N); \forall c \in \mathbb{R}, \phi_{c \cdot u}(i|N) = c \cdot \phi_u(i|N)$.
- (2) **Nullity property:** The dummy player i is defined as a player satisfying $\forall S \subseteq N \setminus \{i\}, v(S \cup \{i\}) = v(S) + v(\{i\})$, which indicates that the player i has no interactions with other players in N , $\phi(i|N) = v(\{i\}) - v(\emptyset)$.
- (3) **Symmetry property:** If $\forall S \subseteq N \setminus \{i, j\}, v(S \cup \{i\}) = v(S \cup \{j\})$, then $\phi(i|N) = \phi(j|N)$.
- (4) **Efficiency property:** The overall reward can be assigned to all players, $\sum_{i \in N} \phi(i|N) = v(N) - v(\emptyset)$.

B. Multi-order Shapley values and interactions

Using Shapley values to explain DNNs. Given a trained DNN and the input with n variables $N = \{1, \dots, n\}$, we can take the input variables as players, and consider the network output as the reward. The Shapley value $\phi(i|N)$ of each input variable $i \in N$ is regarded as the importance of the variable i to the network output. Each subset of variables $S \subseteq N$ represents a specific context. $v(S)$ represents the network output, when we keep variables in S unchanged and mask variables in $N \setminus S$ by following settings in [\(Ancona et al., 2019\)](#). In particular, $v(N)$ refers to the network output *w.r.t.* the entire input N , and $v(\emptyset)$ denotes the output when we mask all variables. Note that for the DNN trained for multi-category classification, $v(S)$ can be taken as an arbitrary dimension of the network output, so as to measure the variable importance to the corresponding category.

B.1. Multi-order Shapley values

This section provides more details about multi-order Shapley values introduced in Section 4.2. We decompose the Shapley value $\phi(i|N)$ into different orders, as follows.

$$\phi(i|N) = \frac{1}{n} \sum_{m=0}^{n-1} \phi^{(m)}(i|N), \quad (9)$$

$$\phi^{(m)}(i|N) = \mathbb{E}_{S \subseteq N \setminus \{i\}, |S|=m} [v(S \cup i) - v(S)], \quad (10)$$

where $\phi^{(m)}(i|N)$ denotes the Shapley value of the m -th order. It measures the importance of the input variable i to the network output with contexts consisting of $m \in \{0, \dots, n-1\}$ variables.

For a low order m , $\phi^{(m)}(i|N)$ denotes the importance of the variable i , when i cooperates with a few contextual variables for inference. For a high order m , $\phi^{(m)}(i|N)$ describes the importance of the variable i , which cooperates with massive contextual variables. In particular, $\phi^{(0)}(i|N) = v(i) - v(\emptyset)$ represents the numerical importance of i without taking into account any contexts.

In addition, we have proven that $\phi^{(m)}(i|N)$ satisfies following properties.

(1) Linearity property: If we merge the outputs of two DNNs $u(S) = w(S) + v(S)$, then the Shapley values of input variables also can be added, *i.e.* $\forall i \in N$, $\phi_u^{(m)}(i|N) = \phi_w^{(m)}(i|N) + \phi_v^{(m)}(i|N)$.

• *Proof:*

$$\begin{aligned}\phi_u^{(m)}(i|N) &= \mathbb{E}_{S \subseteq N \setminus \{i\}, |S|=m} [u(S \cup \{i\}) - u(S)] \\ &= \mathbb{E}_{S \subseteq N \setminus \{i\}, |S|=m} [w(S \cup \{i\}) + v(S \cup \{i\}) - w(S) - v(S)] \\ &= \mathbb{E}_{S \subseteq N \setminus \{i\}, |S|=m} [w(S \cup \{i\}) - w(S)] + \mathbb{E}_{S \subseteq N \setminus \{i\}, |S|=m} [v(S \cup \{i\}) - v(S)] \\ &= \phi_w^{(m)}(i|N) + \phi_v^{(m)}(i|N)\end{aligned}$$

□

(2) Nullity property: An input variable $i \in N$ is considered as a dummy player if $\forall S \subseteq N \setminus \{i\}$, $v(S \cup \{i\}) = v(S) + v(\{i\})$. Thus, the variable i has no interactions with other variables, *i.e.* $\phi^{(m)}(i|N) = v(\{i\})$.

• *Proof:*

$$\begin{aligned}\phi^{(m)}(i|N) &= \mathbb{E}_{S \subseteq N \setminus \{i\}, |S|=m} [v(S \cup \{i\}) - v(S)] \\ &= \mathbb{E}_{S \subseteq N \setminus \{i\}, |S|=m} [v(\{i\})] = v(\{i\})\end{aligned}$$

□

(3) Symmetry property: Given two input variables $i, j \in N$, if these two variables have same cooperations with all other variables $\forall S \subseteq N \setminus \{i, j\}$, $v(S \cup \{i\}) = v(S \cup \{j\})$, then $\phi^{(m)}(i|N) = \phi^{(m)}(j|N)$.

• *Proof:*

$$\begin{aligned}\phi^{(m)}(i|N) &= \mathbb{E}_{S \subseteq N \setminus \{i\}, |S|=m} [v(S \cup \{i\}) - v(S)] \\ &= \frac{m!(n-1-m)!}{(n-1)!} \sum_{S \subseteq N \setminus \{i\}, |S|=m} [v(S \cup \{i\}) - v(S)] \\ &= \frac{m!(n-1-m)!}{(n-1)!} \left(\sum_{S \subseteq N \setminus \{i, j\}, |S|=m-1} [v(S \cup \{i, j\}) - v(S, j)] + \sum_{S \subseteq N \setminus \{i, j\}, |S|=m} [v(S \cup \{i\}) - v(S)] \right) \\ &= \frac{m!(n-1-m)!}{(n-1)!} \left(\sum_{S \subseteq N \setminus \{i, j\}, |S|=m-1} [v(S \cup \{i, j\}) - v(S, i)] + \sum_{S \subseteq N \setminus \{i, j\}, |S|=m} [v(S \cup \{j\}) - v(S)] \right) \\ &= \mathbb{E}_{S \subseteq N \setminus \{j\}, |S|=m} [v(S \cup \{j\}) - v(S)] \\ &= \phi^{(m)}(j|N)\end{aligned}$$

□

(4) Efficiency property: The overall reward can be assigned to all players, $\frac{1}{n} \sum_{i \in N} \sum_{m=0}^{n-1} \phi^{(m)}(i|N) = v(N) - v(\emptyset)$.

• *Proof:*

$$v(N) - v(\emptyset) = \sum_{i \in N} \phi(i|N) = \frac{1}{n} \sum_{i \in N} \sum_{m=0}^{n-1} \phi^{(m)}(i|N)$$

□

B.2. Multi-order interactions

This section provides more details about multi-order interactions in Section 3.

Shapley interaction index. Input variables of a DNN do not contribute to the network output independently. Instead, there are interactions/collaborations between different variables. To this end, the Shapley interaction index (Grabisch & Roubens, 1999) measures the influence of a variable on the Shapley value (importance) of another variable. *I.e.* for two

variables (i, j) , it examines whether the absence/presence of j can change the importance of i . Thus, the Shapley interaction index is defined as the change in the Shapley value (importance) of variable i when the variable j is always present *w.r.t.* the case when j is always absent, as follows.

$$I(i, j) = \tilde{\phi}(i|N)_{j \text{ always present}} - \tilde{\phi}(i|N)_{j \text{ always absent}} \quad (11)$$

where $\tilde{\phi}(i|N)_{j \text{ always present}}$ denotes the Shapley value of the variable i computed under the specific condition that j is always present. $\tilde{\phi}(i|N)_{j \text{ always absent}}$ is computed under the specific condition that j is always absent. Note that $I(i, j) = I(j, i)$. If $I(i, j) > 0$, it indicates that the presence of the variable j will increase the importance of the variable i . Thus, we consider variables (i, j) have a positive interaction. If $I(i, j) < 0$, it indicates a negative interaction.

Multi-order interactions. we propose the multi-order interaction between variables (i, j) , as follows.

$$I_{ij}^{(m)} = \mathbb{E}_{S \subseteq N \setminus \{i, j\}, |S|=m} [\Delta v(i, j, S)], \quad (12)$$

where $\Delta v(i, j, S) \stackrel{\text{def}}{=} v(S \cup \{i, j\}) - v(S \cup \{i\}) - v(S \cup \{j\}) + v(S)$. $I_{ij}^{(m)}$ denotes the interaction of the m -th order, which measures the average interaction between variables (i, j) under all contexts consisting of m variables (*e.g.* visual contexts consisting of m pixels). For a low order m , $I_{ij}^{(m)}$ reflects the interaction between i and j *w.r.t.* simple contextual collaborations with a few variables. For a high order m , $I_{ij}^{(m)}$ corresponds to the interaction *w.r.t.* complex contextual collaborations with massive variables.

We further prove that the Shapley interaction index $I(i, j)$ can be decomposed into interactions of different orders.

$$I(i, j) = \frac{1}{n-1} \sum_{m=0}^{n-2} I_{ij}^{(m)}. \quad (13)$$

• *Proof:*

$$\begin{aligned} I(i, j) &= \tilde{\phi}(i|N)_{j \text{ always present}} - \tilde{\phi}(i|N)_{j \text{ always absent}} \\ &= \frac{1}{n-1} \sum_{m=0}^{n-2} \left(\tilde{\phi}^{(m)}(i|N)_{j \text{ always present}} - \tilde{\phi}^{(m)}(i|N)_{j \text{ always absent}} \right) \\ &= \frac{1}{n-1} \sum_{m=0}^{n-2} \left(\mathbb{E}_{\substack{S \subseteq N \setminus \{i, j\} \\ |S|=m}} [v((S \cup \{j\}) \cup \{i\}) - v(S \cup \{j\})] - \mathbb{E}_{\substack{S \subseteq N \setminus \{i, j\} \\ |S|=m}} [v(S \cup \{i\}) - v(S)] \right) \\ &= \frac{1}{n-1} \sum_{m=0}^{n-2} \left(\mathbb{E}_{S \subseteq N \setminus \{i, j\}, |S|=m} [\Delta v(i, j, S)] \right) = \frac{1}{n-1} \sum_{m=0}^{n-2} I_{ij}^{(m)} \end{aligned}$$

□

We also prove that $I_{ij}^{(m)}$ satisfies *linearity*, *nullity*, *commutativity*, *symmetry*, and *efficiency* properties, which reflect the trustworthiness of the m -order interaction.

(1) Linearity property: If we merge outputs of two DNNs, $u(S) = w(S) + v(S)$, then, $\forall i, j \in N$, the interaction $I_{ij,u}^{(m)}$ *w.r.t.* the new output u can be decomposed into $I_{ij,u}^{(m)} = I_{ij,w}^{(m)} + I_{ij,v}^{(m)}$.

• *Proof:*

$$\begin{aligned} I_{ij,u}^{(m)} &= \mathbb{E}_{S \subseteq N \setminus \{i, j\}, |S|=m} [\Delta u(S, i, j)] \\ &= \mathbb{E}_{S \subseteq N \setminus \{i, j\}, |S|=m} [\Delta v(i, j, S) + \Delta w(S, i, j)] \\ &= I_{ij,v}^{(m)} + I_{ij,w}^{(m)} \end{aligned}$$

□

(2) Nullity property: The dummy variable $i \in N$ satisfies $\forall S \subseteq N \setminus \{i\}, v(S \cup \{i\}) = v(S) + v(\{i\})$. It means that the variable i has no interactions with other variables, *i.e.* $\forall j \in N, I_{ij}^{(m)} = 0$.

• Proof:

$$\begin{aligned}
 I_{ij}^{(m)} &= \mathbb{E}_{S \subseteq N \setminus \{i, j\}, |S|=m} [v(S \cup \{i, j\}) - v(S \cup \{i\}) - v(S \cup \{j\}) + v(S)] \\
 &= \mathbb{E}_{S \subseteq N \setminus \{i, j\}, |S|=m} [v(S \cup \{j\} \cup \{i\}) - v(S \cup \{j\}) - (v(S \cup \{i\}) - v(S))] \\
 &= \mathbb{E}_{S \subseteq N \setminus \{i, j\}, |S|=m} [v(\{i\}) - v(\{i\})] = 0
 \end{aligned}$$

□

(3) **Commutativity property:** $\forall i, j \in N, I_{ij}^{(m)} = I_{ji}^{(m)}$.

• Proof:

$$\begin{aligned}
 I_{ij}^{(m)} &= \mathbb{E}_{S \subseteq N \setminus \{i, j\}, |S|=m} [v(S \cup \{i, j\}) - v(S \cup \{i\}) - v(S \cup \{j\}) + v(S)] \\
 &= \mathbb{E}_{S \subseteq N \setminus \{i, j\}, |S|=m} [v(S \cup \{i, j\}) - v(S \cup \{j\}) - v(S \cup \{i\}) + v(S)] \\
 &= I_{ji}^{(m)}
 \end{aligned}$$

□

(4) **Symmetry property:** If input variables $i, j \in N$ have same cooperations with other variables $\forall S \subseteq N \setminus \{i, j\}, v(S \cup \{i\}) = v(S \cup \{j\})$, then they have same interactions, $\forall k \in N \setminus \{i, j\}, I_{ik}^{(m)} = I_{jk}^{(m)}$.

• Proof:

$$\begin{aligned}
 I_{ik}^{(m)} &= \mathbb{E}_{\substack{S \subseteq N \setminus \{i, j\}, |S|=m}} [\Delta v(i, k, S)] \\
 &= \frac{m!(n-2-m)!}{(n-2)!} \sum_{\substack{S \subseteq N \setminus \{i, k\}, \\ |S|=m}} [\Delta v(i, k, S)] \\
 &= \frac{m!(n-2-m)!}{(n-2)!} \left(\sum_{\substack{S \subseteq N \setminus \{i, j, k\}, \\ |S|=m-1}} [\Delta v(i, k, S \cup \{j\})] + \sum_{\substack{S \subseteq N \setminus \{i, j, k\}, \\ |S|=m}} [\Delta v(i, k, S)] \right) \\
 &= \frac{m!(n-2-m)!}{(n-2)!} \left(\sum_{\substack{S \subseteq N \setminus \{i, j, k\}, \\ |S|=m-1}} [\Delta v(j, k, S \cup \{i\})] + \sum_{\substack{S \subseteq N \setminus \{i, j, k\}, \\ |S|=m}} [\Delta v(j, k, S)] \right) \\
 &= \mathbb{E}_{\substack{S \subseteq N \setminus \{i, j\}, |S|=m}} [\Delta v(j, k, S)] \\
 &= I_{jk}^{(m)}
 \end{aligned}$$

□

(5) **Efficiency property:** The output of the DNN can be decomposed into interactions of different orders, $v(N) = v(\emptyset) + \sum_{i \in N} \phi^{(0)}(i|N) + \sum_{i \in N} \sum_{j \in N \setminus \{i\}} [\sum_{m=0}^{n-2} \frac{n-1-m}{n(n-1)} I_{ij}^{(m)}]$, where $\phi^{(0)}(i|N) \stackrel{\text{def}}{=} v(i) - v(\emptyset)$.

• Proof:

$$\begin{aligned}
 v(N) &= v(\emptyset) + \frac{1}{n} \sum_{i \in N} \sum_{m=0}^{n-1} \phi^{(m)}(i|N) \\
 &= v(\emptyset) + \frac{1}{n} \sum_{i \in N} \phi^{(0)}(i|N) + \frac{1}{n} \sum_{i \in N} \sum_{m=1}^{n-1} \left[\mathbb{E}_{j \in N \setminus \{i\}} \left[\sum_{k=0}^{k=m-1} I_{ij}^{(k)} \right] + \phi^{(0)}(i|N) \right] \\
 &= v(\emptyset) + \sum_{i \in N} \phi^{(0)}(i|N) + \frac{1}{n(n-1)} \sum_{i \in N} \sum_{j \in N \setminus \{i\}} \left[\sum_{m=1}^{n-1} \sum_{k=0}^{k=m-1} I_{ij}^{(k)} \right] \\
 &= v(\emptyset) + \sum_{i \in N} \phi^{(0)}(i|N) + \sum_{i \in N} \sum_{j \in N \setminus \{i\}} \left[\sum_{m=0}^{n-2} \frac{n-1-m}{n(n-1)} I_{ij}^{(m)} \right]
 \end{aligned}$$

B.3. Relationship between multi-order Shapley values and multi-order interactions

We prove that multi-order Shapley values and multi-order interactions satisfy the following *marginal attribution* and *accumulation* properties.

(1) Marginal attribution property: The marginal attribution of the $(m+1)$ -th order Shapley values beyond the m -th order is equal to the average interaction of the m -th order between i and all other variables. $\forall i, j \in N, i \neq j, \phi^{(m+1)}(i|N) - \phi^{(m)}(i|N) = \mathbb{E}_{j \in N \setminus \{i\}}[I_{ij}^{(m)}]$.

• *Proof:*

$$\begin{aligned}
 \phi^{(m+1)}(i|N) - \phi^{(m)}(i|N) &= \mathbb{E}_{\substack{S' \subseteq N \setminus \{i\} \\ |S'|=m+1}} [v(S' \cup \{i\}) - v(S')] - \mathbb{E}_{\substack{S \subseteq N \setminus \{i\} \\ |S|=m}} [v(S \cup \{i\}) - v(S)] \\
 &= \mathbb{E}_{\substack{S \subseteq N \setminus \{i\} \\ |S|=m}} \left[\mathbb{E}_{j \in N \setminus (S \cup \{i\})} [v(S \cup \{j\} \cup \{i\}) - v(S \cup \{j\})] \right] - \mathbb{E}_{\substack{S \subseteq N \setminus \{i\} \\ |S|=m}} [v(S \cup \{i\}) - v(S)] \\
 &= \mathbb{E}_{\substack{S \subseteq N \setminus \{i\} \\ |S|=m}} \left[\mathbb{E}_{j \in N \setminus (S \cup \{i\})} [v(S \cup \{j\} \cup \{i\}) - v(S \cup \{j\}) - v(S \cup \{i\}) + v(S)] \right] \\
 &= \mathbb{E}_{\substack{S \subseteq N \setminus \{i\} \\ |S|=m}} \mathbb{E}_{j \in N \setminus (S \cup \{i\})} [\Delta v(i, j, S)] \\
 &= \mathbb{E}_{j \in N \setminus \{i\}} \mathbb{E}_{\substack{S \subseteq N \setminus \{i, j\} \\ |S|=m}} [\Delta v(i, j, S)] \\
 &= \mathbb{E}_{j \in N \setminus \{i\}} [I_{ij}^{(m)}]
 \end{aligned}$$

□

(2) Accumulation property: The m -th ($m > 0$) order Shapley value of the variable $i \in N$ can be decomposed into interactions of lower orders, $\phi^{(m)}(i|N) = \mathbb{E}_{j \in N \setminus \{i\}}[\sum_{k=0}^{m-1} I_{ij}^{(k)}] + \phi^{(0)}(i|N)$.

• *Proof:*

$$\begin{aligned}
 \phi^{(m)}(i|N) &= \phi^{(m)}(i|N) - \phi^{(m-1)}(i|N) + \phi^{(m-1)}(i|N) - \phi^{(m-2)}(i|N) + \cdots - \phi^{(0)}(i|N) + \phi^{(0)}(i|N) \\
 &= \mathbb{E}_{j \in N \setminus \{i\}}[I_{ij}^{(m-1)}] + \mathbb{E}_{j \in N \setminus \{i\}}[I_{ij}^{(m-2)}] + \cdots + \mathbb{E}_{j \in N \setminus \{i\}}[I_{ij}^{(0)}] + \phi^{(0)}(i|N) \\
 &= \mathbb{E}_{j \in N \setminus \{i\}} \left[\sum_{k=0}^{k=m-1} I_{ij}^{(k)} \right] + \phi^{(0)}(i|N)
 \end{aligned}$$

□

B.4. Equivalence between the multi-order interaction and the mutual information

When a DNN outputs a probability distribution, we prove that its interaction can be represented in the form of mutual information. Without loss of generality, let us take the image classification task for example. Let $x \in X \subseteq \mathbb{R}^n$ denote the input image of the DNN. x_i denotes the i -th pixel, and $X_i = \{x_i\}$. $\forall S \subseteq N$, we define $X_S = \{x_S | x \in X\}$; each x_S represents the image, where pixels in S remain unchanged, and other pixels $j \in N \setminus S$ are masked following settings of (Ancona et al., 2019). Let $y \in Y = \{y^1, \dots, y^C\}$ denote the network prediction. In this way, given x_S as the input, $p(y|x_S)$ denotes the output probability of the DNN. Let us set $v(S) = H(Y|X_S) = \sum_{x_S} p(x_S)H(Y|X_S = x_S)$, which measures the entropy of y given the input x_S . Then we prove that

$$I_{ij}^{(m)} = \mathbb{E}_{S \subseteq N \setminus \{i, j\}, |S|=m} MI(X_i; X_j; Y|X_S) \quad (14)$$

• *Proof:*

$$\begin{aligned}
 I_{ij}^{(m)} &= \mathbb{E}_{S \subseteq N \setminus \{i, j\}, |S|=m} \left[v(S \cup \{i, j\}) - v(S \cup \{i\}) - v(S \cup \{j\}) + v(S) \right] \\
 &= \mathbb{E}_{S \subseteq N \setminus \{i, j\}, |S|=m} \left[-H(Y|X_S, X_i, X_j) + H(Y|X_S, X_i) + H(Y|X_S, X_j) - H(H|X_S) \right] \\
 &= \mathbb{E}_{S \subseteq N \setminus \{i, j\}, |S|=m} \left[H(Y|X_S, X_j) - H(Y|X_S, X_j, X_i) + H(Y|X_S, X_i) - H(Y|X_S) \right] \\
 &= \mathbb{E}_{S \subseteq N \setminus \{i, j\}, |S|=m} \left[MI(X_i; Y|X_S, X_j) - MI(X_i; Y|X_S) \right] \\
 &= \mathbb{E}_{S \subseteq N \setminus \{i, j\}, |S|=m} \left[MI(X_i; X_j; Y|X_S) \right]
 \end{aligned}$$

□

When X_S (with m pixels) is given, we can roughly understand the conditional mutual information $MI(X_{\{i,j\}}; Y|X_S)$ as the additional benefits from X_i and X_j to classification. We prove that

$$MI(X_{\{i,j\}}; Y|X_S) = MI(X_i; Y|X_j, X_S) + MI(X_j; Y|X_i, X_S) + MI(X_i; X_j; Y|X_S) \quad (15)$$

• *Proof:*

$$\begin{aligned} \text{right} &= MI(X_i; Y|X_j, X_S) + MI(X_j; Y|X_i, X_S) + MI(X_i; X_j; Y|X_S) \\ &= MI(X_i; Y|X_j, X_S) + MI(X_j; Y|X_i, X_S) + MI(X_i; Y|X_S) - MI(X_i; Y|X_j, X_S) \\ &= MI(X_i; Y|X_j, X_S) + MI(X_i; Y|X_S) \\ &= \sum_{x_i, x_j, x_S, y} p(x_i, x_j, x_S, y) \log \frac{p(x_j, y|x_i, x_S)}{p(x_j|x_i, x_S)p(y|x_i, x_S)} + \sum_{x_i, x_S, y} p(x_i, x_S, y) \log \frac{p(x_i, y|x_S)}{p(x_i|x_S)p(y|x_S)} \\ &= \sum_{x_i, x_j, x_S, y} p(x_i, x_j, x_S, y) \log \frac{p(x_j, y|x_i, x_S)}{p(x_j|x_i, x_S)p(y|x_i, x_S)} + \sum_{x_i, x_j, x_S, y} p(x_i, x_j, x_S, y) \log \frac{p(x_i, y|x_S)}{p(x_i|x_S)p(y|x_S)} \\ &= \sum_{x_i, x_j, x_S, y} p(x_i, x_j, x_S, y) \log \frac{p(x_j, y|x_i, x_S)p(x_i, y|x_S)}{p(x_j|x_i, x_S)p(y|x_i, x_S)p(x_i|x_S)p(y|x_S)} \\ &= \sum_{x_i, x_j, x_S, y} p(x_i, x_j, x_S, y) \log \frac{p(x_j, y|x_i, x_S)p(x_i, y|x_S)p(x_i, x_S)p(x_S)}{p(x_j|x_i, x_S)p(y|x_i, x_S)p(x_i|x_S)p(y|x_S)p(x_i, x_S)p(x_S)} \\ &= \sum_{x_i, x_j, x_S, y} p(x_i, x_j, x_S, y) \log \frac{p(x_i, x_j, x_S, y)p(x_i, x_S, y)}{p(x_j|x_i, x_S)p(x_i, x_S, y)p(x_i|x_S)p(y|x_S)p(x_S)} \\ &= \sum_{x_i, x_j, x_S, y} p(x_i, x_j, x_S, y) \log \frac{p(x_i, x_j, x_S, y)}{p(x_j|x_i, x_S)p(x_i|x_S)p(y|x_S)p(x_S)} \\ &= \sum_{x_i, x_j, x_S, y} p(x_i, x_j, x_S, y) \log \frac{p(x_i, x_j, y|x_S)}{p(x_i, x_j|x_S)p(y|x_S)} \\ &= MI(X_{\{i,j\}}; Y|X_S) = \text{left} \end{aligned}$$

□

C. Information reflected by $\Delta I^{(m)}$

In section 4.1 of the paper, we propose the metric $I^{(m)} = \mathbb{E}_{x \in \Omega} \mathbb{E}_{i,j} [I_{ij}^{(m)}(x)]$, and $\Delta I^{(m)} \stackrel{\text{def}}{=} I_{\text{nor}}^{(m)} - I_{\text{adv}}^{(m)}$, which measures the difference in interactions between normal samples and adversarial examples. In this section ,we prove

$$\Delta I^{(m)} = \mathbb{E}_{x \in \Omega} \mathbb{E}_{i,j} [\Delta I_{ij}^{(m)}(x)] \quad (16)$$

where $\Delta I_{ij}^{(m)}(x) = I_{ij}^{(m)}(x) - I_{ij}^{(m)}(\tilde{x})$.

• *Proof:*

$$\begin{aligned} \Delta I^{(m)} &= I_{\text{nor}}^{(m)} - I_{\text{adv}}^{(m)} \\ &= \mathbb{E}_{x \in \Omega_{\text{nor}}} \mathbb{E}_{i,j} [I_{ij}^{(m)}(x)] - \mathbb{E}_{x \in \Omega_{\text{adv}}} \mathbb{E}_{i,j} [I_{ij}^{(m)}(x)] \\ &= \mathbb{E}_{x \in \Omega_{\text{nor}}} \mathbb{E}_{i,j} [I_{ij}^{(m)}(x)] - \mathbb{E}_{x \in \Omega_{\text{nor}}} \mathbb{E}_{i,j} [I_{ij}^{(m)}(x + \Delta x)] \\ &= \mathbb{E}_{x \in \Omega_{\text{nor}}} \mathbb{E}_{i,j} [I_{ij}^{(m)}(x) - I_{ij}^{(m)}(x + \Delta x)] \\ &= \mathbb{E}_{x \in \Omega_{\text{nor}}} \mathbb{E}_{i,j} [I_{ij}^{(m)}(x) - I_{ij}^{(m)}(\tilde{x})] \\ &= \mathbb{E}_{x \in \Omega_{\text{nor}}} \mathbb{E}_{i,j} [\Delta I_{ij}^{(m)}(x)] \end{aligned}$$

□

D. The attribution-based method of detecting adversarial examples

This section provides more details about the attribution-based method of detecting adversarial examples discussed in Section 4.2 of the paper.

Yang et al. (2019) proposed an attribution-based method to detect adversarial examples, which used the attribution score of input variables. The attribution score of the variable i in (Yang et al., 2019) is defined as

$$\phi(x)_i := f(x)_c - f(x_{(i)})_c, \text{ where } c = \arg \max_{j \in C} f(x)_j \quad (17)$$

where x denotes the original input sample, and $x_{(i)}$ denotes the input sample with the i -th variable masked by 0. $f(x)_c$ denotes the network output of the c -th category. Actually, $f(x)_c$ can also be written as $v(N|x)$, and $f(x_{(i)})_c$ can be written as $v(N \setminus \{i\}|x)$. Thus, the attribution score can be represented as $v(N|x) - v(N \setminus \{i\}|x)$. We prove that $v(N|x) - v(N \setminus \{i\}|x) = \phi^{(n-1)}(i|N, x)$.

• *Proof:*

$$\begin{aligned} v(N|x) - v(N \setminus \{i\}|x) &= v((N \setminus \{i\}) \cup \{i\}|x) - v(N \setminus \{i\}|x) \\ &= v(S \cup \{i\}|x) - v(S|x) \quad \% S \stackrel{\text{def}}{=} N \setminus \{i\}, |S| = n - 1 \\ &= \mathbb{E}_{S \subseteq N \setminus \{i\}, |S|=n-1} [v(S \cup \{i\}|x) - v(S|x)] \\ &= \phi^{(n-1)}(i|N, x) \end{aligned}$$

□

According to the *accumulation property* of multi-order Shapley values and interactions, we have $\phi^{(n-1)}(i|N, x) = \mathbb{E}_{j \in N \setminus \{i\}} \left[\sum_{m=0}^{n-2} I_{ij}^{(m)} \right] + \phi^{(0)}(i|N, x)$. This indicates that $\phi^{(n-1)}(i|N, x)$ contains the interaction components with the highest order ($m = n - 2$), which are not included in Shapley values with orders lower than $n - 1$. Section 4.1 of the paper has pointed that high-order interactions are the most sensitive to adversarial perturbations, thereby enabling the detection of adversarial examples.

E. Effectiveness of the dropout method to correct network output of adversarial examples

In this section, we theoretically prove the effectiveness of the dropout method in Section 4.5. Specifically, we prove that the dropout operation on the input sample can remove high-order interactions, which are sensitive to adversarial attacks.

Given the input sample $x \in \mathbb{R}^n$ and the dropout ratio α , let $\mathcal{K} = \{K|K \subset N, |K| = \lfloor (1 - \alpha)n \rfloor\}$ denote all possible sets of remained variables after the dropout operation. Let $v^\alpha(N|x) = \mathbb{E}_{K \in \mathcal{K}} [v(K|x)]$ denote the average network output among all inputs after the dropout operation with rate α . According to the efficiency property of the multi-order interaction, we have

$$v(N|x) = v(\emptyset|x) + \sum_{i \in N} \phi^{(0)}(i|N, x) + \sum_{i \neq j \in N} \sum_{m=0}^{n-2} \frac{n-1-m}{n(n-1)} I_{ij, N}^{(m)}(x) \quad (18)$$

where $I_{ij, N}^{(m)}(x)$ denotes the m -order interaction between variables (i, j) of the input x with all variables N . Similarly,

$$v(K|x) = v(\emptyset|x) + \sum_{i \in K} \phi^{(0)}(i|K, x) + \sum_{i \neq j \in K} \sum_{m=0}^{k-2} \frac{k-1-m}{k(k-1)} I_{ij, K}^{(m)}(x) \quad (19)$$

where $k = |K| = \lfloor (1 - \alpha)n \rfloor$. Thus,

$$\begin{aligned}
 v^\alpha(N|x) &= \mathbb{E}_{K \in \mathcal{K}}[v(K|x)] \\
 &= \mathbb{E}_{K \in \mathcal{K}} \left[v(\emptyset|x) + \sum_{i \in K} \phi^{(0)}(i|K, x) + \sum_{i \neq j \in K} \sum_{m=0}^{k-2} \frac{k-1-m}{k(k-1)} I_{ij,K}^{(m)}(x) \right] \\
 &= v(\emptyset|x) + \mathbb{E}_{K \in \mathcal{K}} \left[\sum_{i \in K} (v(i|x) - v(\emptyset|x)) \right] + \mathbb{E}_{K \in \mathcal{K}} \left[\sum_{i \neq j \in K} \sum_{m=0}^{k-2} \frac{k-1-m}{k(k-1)} I_{ij,K}^{(m)}(x) \right] \\
 &= v(\emptyset|x) + \mathbb{E}_{\substack{K \subset N \\ k=(1-\alpha)n}} \left[\sum_{i \in K} \phi^{(0)}(i|N, x) \right] + \mathbb{E}_{\substack{K \subset N \\ k=(1-\alpha)n}} \left[\sum_{i \neq j \in K} \sum_{m=0}^{k-2} \frac{k-1-m}{k(k-1)} I_{ij,K}^{(m)}(x) \right] \\
 &= v(\emptyset|x) + (1 - \alpha) \sum_{i \in N} \phi^{(0)}(i|N, x) + \mathbb{E}_{\substack{K \subset N \\ k=(1-\alpha)n}} \left[\sum_{i \neq j \in K} \sum_{m=0}^{k-2} \frac{k-1-m}{k(k-1)} I_{ij,K}^{(m)}(x) \right] \\
 &= v(\emptyset|x) + (1 - \alpha) \sum_{i \in N} \phi^{(0)}(i|N, x) + \mathbb{E}_{\substack{K \subset N \\ k=(1-\alpha)n}} \left[\sum_{i \neq j \in K} \sum_{m=0}^{k-2} \frac{k-1-m}{k(k-1)} \mathbb{E}_{\substack{S \subseteq K \setminus \{i,j\} \\ |S|=m}} [\Delta v(i, j, S|x)] \right] \\
 &= v(\emptyset|x) + (1 - \alpha) \sum_{i \in N} \phi^{(0)}(i|N, x) + \frac{k(k-1)}{n(n-1)} \sum_{i \neq j \in N} \sum_{m=0}^{k-2} \frac{k-1-m}{k(k-1)} \mathbb{E}_{\substack{K \subset N \\ k=(1-\alpha)n}} \mathbb{E}_{\substack{S \subseteq K \setminus \{i,j\} \\ |S|=m}} [\Delta v(i, j, S|x)] \\
 &= v(\emptyset|x) + (1 - \alpha) \sum_{i \in N} \phi^{(0)}(i|N, x) + \sum_{i \neq j \in N} \sum_{m=0}^{k-2} \frac{k-1-m}{n(n-1)} \mathbb{E}_{\substack{S \subseteq N \setminus \{i,j\} \\ |S|=m}} [\Delta v(i, j, S|x)] \\
 &= v(\emptyset|x) + (1 - \alpha) \sum_{i \in N} \phi^{(0)}(i|N, x) + \sum_{i \neq j \in N} \sum_{m=0}^{k-2} \frac{k-1-m}{n(n-1)} I_{ij,N}^{(m)}(x) \\
 \end{aligned} \tag{20}$$

Thus, the change in the network output caused by the dropout operation can be represented as follows,

$$\begin{aligned}
 v(N|x) - v^\alpha(N|x) &= \alpha \sum_{i \in N} \phi^{(0)}(i|N, x) + \sum_{i \neq j \in N} \left[\sum_{m=0}^{n-2} \frac{n-1-m}{n(n-1)} I_{ij,N}^{(m)}(x) - \sum_{m=0}^{k-2} \frac{k-1-m}{n(n-1)} I_{ij,N}^{(m)}(x) \right] \\
 &= \alpha \sum_{i \in N} \phi^{(0)}(i|N, x) + \sum_{i \neq j \in N} \sum_{m=0}^{k-2} \frac{n-k}{n(n-1)} I_{ij,N}^{(m)}(x) + \sum_{i \neq j \in N} \sum_{m=k-1}^{n-2} \frac{n-1-m}{n(n-1)} I_{ij,N}^{(m)}(x) \\
 &= \alpha \sum_{i \in N} \phi^{(0)}(i|N, x) + \frac{\alpha}{n-1} \sum_{i \neq j \in N} \sum_{m=0}^{k-2} I_{ij,N}^{(m)}(x) + \underbrace{\sum_{i \neq j \in N} \sum_{m=k-1}^{n-2} \frac{n-1-m}{n(n-1)} I_{ij,N}^{(m)}(x)}_{\text{high-order interactions}}
 \end{aligned} \tag{21}$$

According to Eq. (21), the dropout operation removes all high-order interactions ($m > (1 - \alpha)n - 2$), while slightly affects low-order interactions. Thus, the dropout operation can remove sensitive interaction components of the DNN, thereby reducing the attacking utility of perturbations and correcting the network output.

F. Experimental results

F.1. Experimental results based on other attacking methods

Besides the ℓ_∞ PGD attacks (Madry et al., 2018), we also conducted experiments on other attacking methods (Dong et al., 2018). Figure 6 shows experimental results on the MI attack, which also verify our conclusions. Note that the attacking

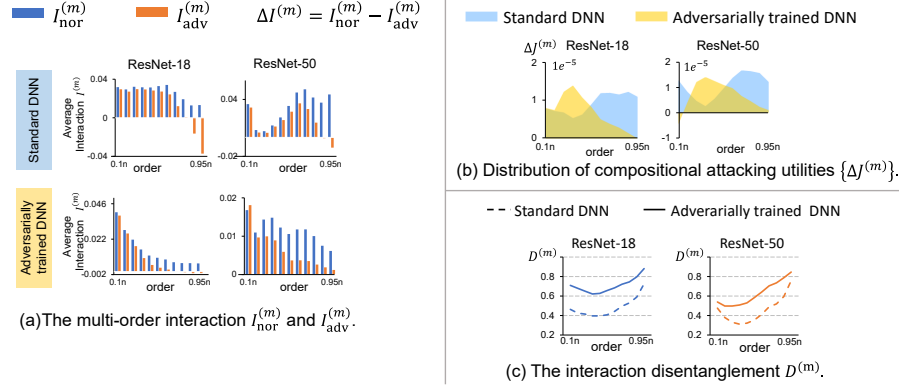


Figure 6. Experimental results on ResNet-18/50 w.r.t. the untargeted MI attack (Dong et al., 2018).

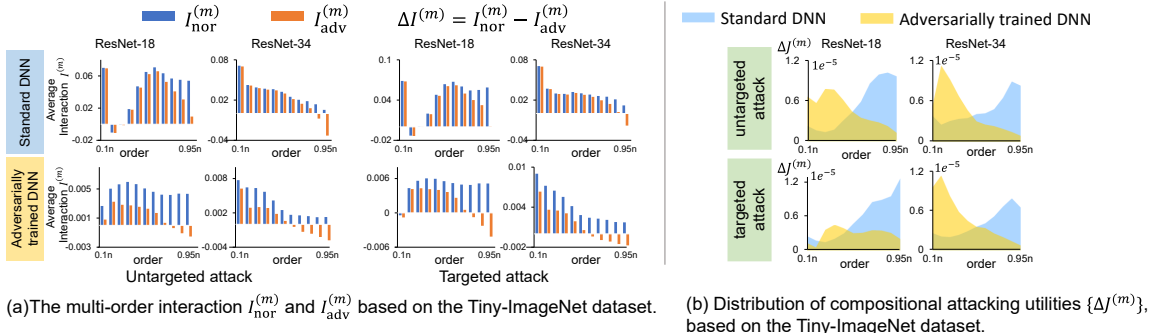


Figure 7. Interactions and attacking utilities based on the Tiny-ImageNet dataset.

utility on high/middle-order interactions may make $\Delta J^{(m)}$ on low-order interactions negative, as a trade-off.

F.2. Results based on the Tiny-ImageNet dataset

This section provides experimental results based on the Tiny-ImageNet dataset. Figure 7 (a) shows $I_{\text{nor}}^{(m)}$ and $I_{\text{adv}}^{(m)}$ of different orders w.r.t. the ground-truth category. Similar to results based on the ImageNet dataset, adversarial perturbations significantly decreased high-order interactions, in both adversarially trained DNNs and standard DNNs. Figure 7 (b) shows the distribution of compositional attacking utilities of multi-order interactions, i.e. $J^{(m)} = \frac{n-1-m}{n(n-1)} I^{(m)}$. Compared to standard DNNs, low/middle-order interactions of adversarially trained DNNs took up more attacking utility. Besides, high-order interactions in adversarially trained DNNs were more robust than those of standard DNNs.

F.3. Analysis about interactions w.r.t. the target category and other categories

This section analyzes the interactions w.r.t. the target category and other categories. In the targeted attack, the target category was referred to as the target label. In the untargeted attack, we considered the misclassified category as the target category. Given each input image, we measured the interaction w.r.t. the output of its target category by setting $v(S|x) = \log p(y = y^{\text{target}}|S, x)$. Besides, we also measured the interactions w.r.t. outputs of other categories, except the ground-truth category.

Considering the softmax operation $p(y = y^{\text{truth}}|S, x) = \frac{\exp(h_{y^{\text{truth}}}(S|x))}{\sum_{y'} \exp(h_{y'}(S|x))}$, we set $v(S|x) = \log \sum_{y' \neq y^{\text{truth}}} \exp(h_{y'}(S|x))$ to measure the interaction w.r.t. effects on other categories. $h_{y'}(S|x)$ denoted the network output of the category y' before the softmax layer, when we took variables in S of x as the input. Figure 8 shows interactions w.r.t. outputs of the target category and other categories. We found that high-order interactions w.r.t. other categories usually increased. Meanwhile, high-order interactions w.r.t. the target category also significantly increased. This indicated that adversarial perturbations adversely affected complex features corresponding to the ground-truth category, while encouraging features for other categories, especially for the target category.

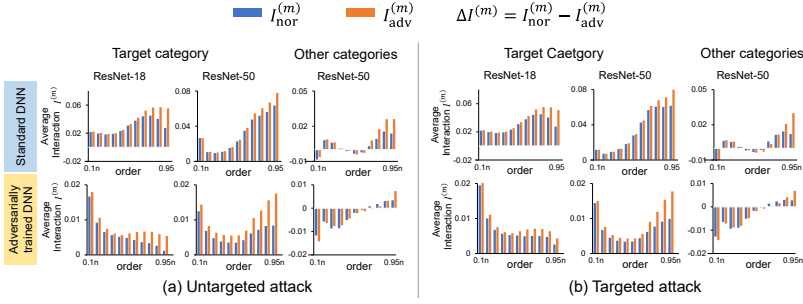
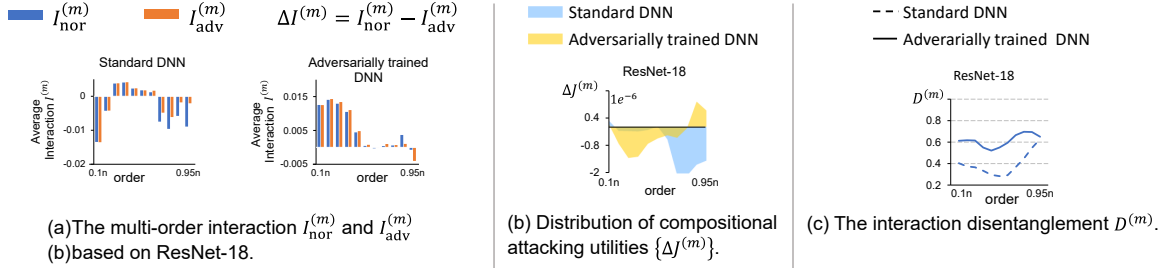


Figure 8. Interactions w.r.t. the target category and other categories.

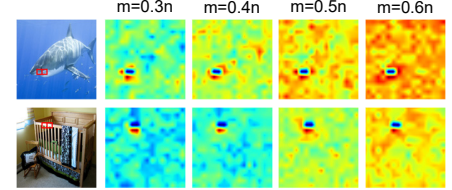

 Figure 10. Experimental results on ResNet-18 w.r.t. untargeted attacks when we set $\hat{v}(S) = H(Y|X_S)$.

F.4. Visualization results based on ResNet-50

This section provides visualization results of interaction contexts based on the standardly trained ResNet-50. As shown in Figure 9, low-order interactions usually represented simple features of local collaborations, and high-order interactions usually reflected complex features of global collaborations.

F.5. Verification of conclusions when $\hat{v}(S) = H(Y|X_S)$

In Eq. (4) of the paper, we set $\hat{v}(S) = H(Y|X_S)$, which is slightly different from setting $v(S) = \log p(y = y^{\text{truth}}|S, x)$ in Section 4.1. Nevertheless, the trend of $v(S)$ can roughly reflect the negative trend of $\hat{v}(S)$. Crucially, we also measured the change of multi-order interaction strength using $\hat{v}(S)$. As Figure 10 shows, we obtained the same conclusion, *i.e.* high-order interactions in adversarially trained DNNs were more robust in those in standard DNNs.


 Figure 9. Contexts of the m -order interaction $I_{ij}^{(m)}$ in normal samples of standard ResNet-50.